Meson decays by flux-tube breaking

Richard Kokoski and Nathan Isgur
Department of Physics, University of Toronto, Toronto, Canada M5S 1A7
(Received 7 October 1985)

We have examined meson decays in a model with chromoelectric flux-tube breaking motivated by the strong-coupling limit of QCD. Our analysis includes all of the simple decay modes of mesons with up to two units of orbital or one unit of radial excitation, as well as a number of other interesting modes and higher-mass resonances. In conjunction with the wave functions of a relativized version of the quark model, our calculations provide, in terms of a single elementary flux-tube-breaking amplitude, predictions for meson decay amplitudes which are in excellent correspondence to experiment. The model also (1) leads to an understanding of the relevance and success of the $^3P_0$ model, (2) provides predictions for channels in which it should be possible to see many of the missing low-lying mesons of the quark model, (3) points toward solutions to some puzzles in meson phenomenology, and (4) promises to be a useful tool for understanding the properties of unconventional mesons, especially meson hybrids.

I. INTRODUCTION

Quantum chromodynamics (QCD) promises to eventually provide a complete understanding of strong-interaction phenomena, and indeed much progress in understanding hadrons via QCD has already been made. Especially noteworthy are the recent demonstrations, using numerical lattice-gauge-theory methods, that QCD confines. We can hope that in the future such techniques will lead to *ab initio* calculations of hadronic masses and properties.

Even if these advances occur relatively soon, but especially if they do not, it is useful to build models for QCD which we can use both to study phenomena beyond the scope of contemporary computing capacity and also as a tool for interpreting the raw output of the first-principles numerical calculations. The quark model, especially when supplemented with dynamics suggested by QCD, is a prime example of such a model.

We believe that a recent extension[1] of the quark model to include gluonic degrees of freedom holds considerable promise for expanding our ability to predict and interpret the complex character of hadrons in QCD. This "flux-tube model" for QCD is based on the strong-coupling Hamiltonian lattice formulation of the theory[2] in which the basic degrees of freedom are most conveniently taken to be quarks and flux tubes rather than quarks and gluons. In this paper we describe the application of the flux-tube model to the decays of $q\bar{q}$ states.

Models for the strong decays of hadrons have a long history.[3-5] Within the context of the quark model, such analyses began[3] by avoiding explicit description of the decay process itself: they examined only those general properties following from various symmetries such as SU(6) and $SU(6)_W$. More explicit[3] are models in which an "elementary" meson is emitted by a single quark, and such models have proved to be very useful. More fundamental are the quark-pair-creation models,[4] which treat all of the hadrons participating in the decay process on an equal footing.

The $^3P_0$ quark-pair-creation model, which has been very impressively developed and exploited in applications to both mesons and baryons,[5] will turn out to be related to the flux-tube-breaking model[6] which we discuss here: it will emerge as a limiting case of our model when the flux-tube wave function is much more extended than the quark-antiquark wave function. Although this limit is not realistic, it so happens that in many simple situations there is still a strong correspondence between the results of the two models; the reasons for this will be discussed below.

II. DECAYS IN THE FLUX-TUBE MODEL

The flux-tube model of Ref. 1 is based on the strong-coupling Hamiltonian lattice formulation[2] of QCD. In the limit $g \to \infty$, the eigenstates of quantum chromodynamics consist of "frozen" configurations of quarks and flux links (or flux tubes) connected on a lattice with lattice spacing a in arbitrary ways consistent with local SU(3) gauge invariance. The "primitive meson" sector, for example, corresponds in this limit to states with a quark and antiquark (at arbitrary points in the lattice) connected by arbitrary configurations of chromoelectric flux along the links between lattice points as in Fig. 1(a). Some primitive states of the baryon and pure glue sectors are shown in Fig. 1(b) and 1(c). For $g < \infty$, these $g \to \infty$ eigenstates remain a complete set of basis states for QCD, but they become perturbed by two types of interactions. The first of these takes the form

$$\sum_{\text{links } l_{ji}} q_j^\dagger U_{ji} \alpha_{ji} q_i \ ,$$

where q_n is the quark field operator at the lattice site n, U_{ji} creates a unit of three-flux on the "link" from j to i (or destroys a unit of three-flux from i to j), and α_{ji} is the

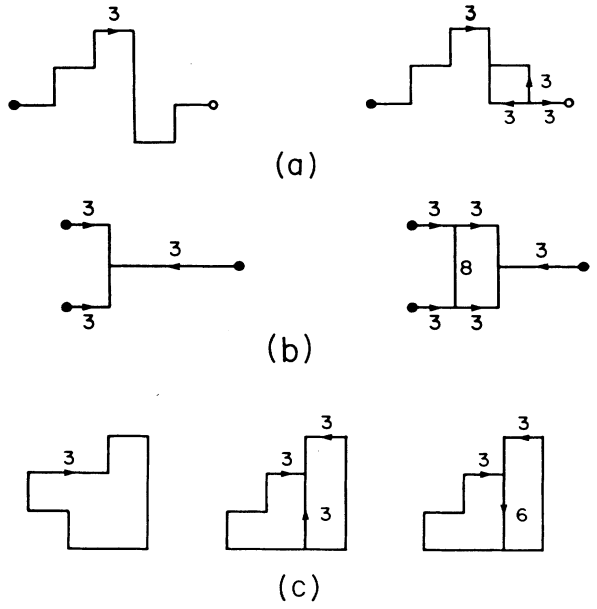

FIG. 1. (a) Some primitive meson states; (b) some primitive baryon states; (c) some primitive pure glue states.

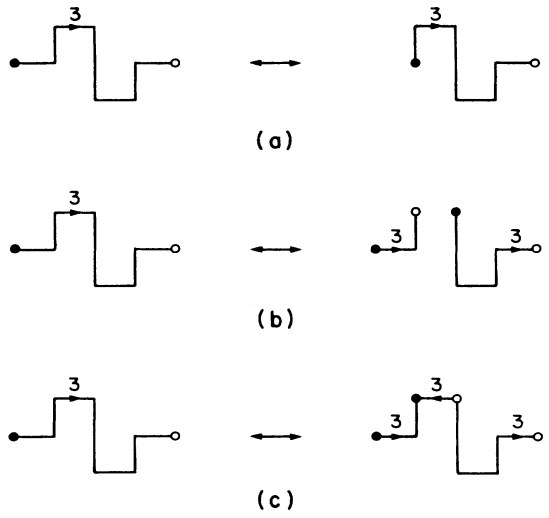

FIG. 2. Some effects of $q^{\dagger}U\alpha q$: (a) quark hopping, (b) flux-breaking pair creation, (c) $q\bar{q}$ "seeding."

Dirac matrix in the direction of the link l_{ji}. The second has the form

$$\sum_{\substack{\text{plaquettes}\\ p(l_4 l_3 l_2 l_1)}} \mathrm{Tr}(U_{l_4}U_{l_3}U_{l_2}U_{l_1}+\mathrm{H.c.})\ ,$$

where a plaquette is an elementary square in the lattice with the links l_1,l_2,l_3,l_4 on its border. This term can therefore create or destroy a unit "loop" of three-flux around any plaquette. Some examples of the action of these two perturbations are given in Figs. 2 and 3.

To recover QCD from lattice QCD, one must let the lattice spacing become small; in this process the bare coupling g must, according to the lattice renormalization-group equations, also become small so that the above-mentioned perturbations of the strong-coupling-limit eigenstates become important. The flux-tube model of Ref. 1 is based on the hypothesis that it is useful to diagonalize this problem in blocks of states of the same topology and to then consider mixing between these topological sectors. Thus initially one considers only quark and flux-tube "hopping" effects which unfreeze the states of the $g\rightarrow\infty$ limit but will not, for example, mix a $q\bar{q}$ meson with a simple three-flux with one which has a bubble or with a $q\,q\,\bar{q}\,\bar{q}$ state. The problem of the diagonalization of the topological blocks is then the normal mode problem for the various quark and "string" configurations. A heavy $Q\bar{Q}$ meson, for example, corresponds in this approximation to a quark and antiquark moving in the (adiabatic) potential of the ground state of the elementary three-flux. The corresponding hybrid mesons correspond to states with "phonon" excitations in the flux tube or (at higher masses) with more complicated flux-tube topologies, and so on. This "quark-model limit" can then be systematically improved by considering corrections to the adiabatic limit and by considering the topologically nondiagonal effects of the perturbations $q^{\dagger}U\alpha q$ and $\mathrm{Tr}(UUUU+\mathrm{H.c.})$.

In this paper we will be concentrating on the topological mixing caused by the pair-creation/flux-tube-annihilation part of the $q^{\dagger}U\alpha q$ term which causes the decay of ordinary mesons. We begin by extracting a plausible model for this process from the strong-coupling expansion.

For large g (and therefore large a), pair creation is

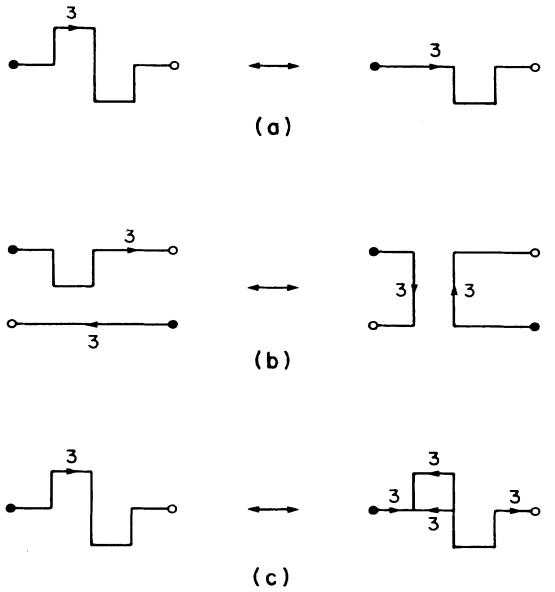

FIG. 3. Some effects of $\mathrm{Tr}(U_4U_3U_2U_1+\mathrm{H.c.})$: (a) flux-tube hopping, (b) flux-tube topological mixing by rearrangement, (c) flux-tube topological mixing by "bubble formation."

unimportant; it is also weak for $a \to 0$ since in this limit $g \to 0$. It is therefore plausible that quark-pair creation is an intermediate range process which can be effectively studied using a lattice spacing a_1 with $g(a_1) \sim 1$ by treating the $q^\dagger U \alpha q$ term as an effective lowest-order interaction.

When a meson flux tube is broken [as in Fig. 2(b)] by pair creation on a link from $\mathbf{n}$ to $\mathbf{n}+\hat{\mathbf{e}}$, the resulting quark pair is created with an effective operator

$$C_{\mathbf{n},\hat{\mathbf{e}}} = \frac{3\gamma(\mathbf{n})}{a} \sum_q \mathbf{q}^\dagger(\mathbf{n}) \boldsymbol{\alpha} \cdot \hat{\mathbf{e}} q(\mathbf{n}+\hat{\mathbf{e}}) , \tag{1}$$

where $\gamma(\mathbf{n})$ depends on the string state of the meson. Note that the quark colors are automatically correct (a factor of $\frac{1}{3}$ arises from requiring that the flux on the link couples to a singlet, but we have inserted a factor of 9 for later convenience) and that this elementary creation amplitude is flavor symmetric. If we expand

$$q(\mathbf{n}+\hat{\mathbf{e}}) \simeq q(\mathbf{n}) + a_1 \hat{\mathbf{e}} \cdot \nabla q(\mathbf{n}) ,$$

then

$$C_{\mathbf{n},\hat{\mathbf{e}}} = \frac{3\gamma(\mathbf{n})}{a_1} \sum_q q^\dagger(\mathbf{n}) \alpha \cdot \hat{\mathbf{e}} q(\mathbf{n}) + 3\gamma(\mathbf{n}) \sum_q q^\dagger(\mathbf{n}) \alpha \cdot \hat{\mathbf{e}} \hat{\mathbf{e}} \cdot \nabla q(\mathbf{n}) + \cdots . \tag{2}$$

Up to this point our physical picture is very similar to that of Ref. 7. However, in Ref. 7 $\hat{\mathbf{e}}$ is taken to be parallel to the initial meson radius vector $\mathbf{r} = \mathbf{r}_q - \mathbf{r}_{\bar{q}}$. We believe this to be incorrect. On a scale $\lesssim a_1$, the string is not straight since it is subject to "roughening": the string is executing zero-point oscillations of all of its normal modes which range from wavelengths $r/2$ down to scales near a_1 [where because $g(a_1) = 1$, the simple string picture becomes modified by topological mixing]. Thus we should expect the piece of flux cut out at the small scale a_1 to be *unoriented* and we should average over $\hat{\mathbf{e}}$. Since $\langle \boldsymbol{\alpha} \cdot \hat{\mathbf{e}} \rangle = 0$ and $\langle \hat{\mathbf{e}}_i \hat{\mathbf{e}}_j \rangle = \frac{1}{3}\delta_{ij}$ we therefore obtain

$$C_{\mathbf{n}} \simeq \gamma(\mathbf{n}) \sum_q q^\dagger(\mathbf{n}) \boldsymbol{\alpha} \cdot \nabla q(\mathbf{n}) . \tag{3}$$

(We will test and confirm this argument for the lack of orientation of $\hat{\mathbf{e}}$ in the phenomenological discussions of Sec. III below.) Since this operator is invariant under rotations about the point $\mathbf{n}$ and has positive parity, it produces a quark-antiquark pair in a $^3P_0$ state. If we were to assume that $\gamma(\mathbf{n})$ is independent of $\mathbf{n}$, we would then begin to recover the naive $^3P_0$ pair-creation model. Of course, in our picture it is not: $\gamma(\mathbf{n})$ will be nonzero only in the region between the quark and antiquark where the string wave function is nonzero; moreover, the full amplitude for the string-breaking transition in question will depend not only on a quark-wave-function overlap, but also on the amplitude to find the broken string in the string wave functions of the final-state mesons. In Appendix A we show that when a mesonic ground-state string breaks into two other mesonic strings in their ground states, one obtains (in the small oscillations approximation) a string overlap function

$$\gamma_{00}^0(\mathbf{n}) \propto \exp[-\tfrac{1}{2} f(\xi) b y_\perp^2] , \tag{4}$$

where $\mathbf{n}a = \mathbf{r}_{\bar{q}} + \xi \mathbf{r} + \mathbf{y}_\perp$ with $\mathbf{y}_\perp$ a transverse vector from the equilibrium position $\mathbf{r}_{\bar{q}} + \xi \mathbf{r}$ of the string ($0 \le \xi \le 1$) to the point where the break occurs [see Fig. 4(a)], b is the string tension, and $f(\xi)$ is a ξ-dependent coefficient of order unity. In the string-breaking model the pair creation thus tends to occur in a cylindrical region with radius $O(b^{-1/2})$ about the $q\bar{q}$ axis. Of course the form (4) is only correct for the stated process; when, for example, the excited string of a hybrid meson breaks, a different overlap function results. We comment on this point further in a concluding section.

For our actual calculations, after checking that our results were insensitive to $f(\xi)$ for $\frac{1}{3} < f < 3$, we approximated the complicated ξ dependence of (4) by the simpler ξ-independent form:

$$\gamma_{00}^0(\mathbf{n}) = \gamma_0 e^{-(b/2) w_{\min}^2} , \tag{5}$$

where $w_{\min}$ is the shortest distance from the pair-creation point $\mathbf{n}$ to the line between the quark and antiquark (thus $w_{\min} = y_\perp$ for $0 \le \xi \le 1$). This leads to a cigar-shaped pair-creation region, as illustrated in Fig. 4(b).

A decay amplitude $A \to BC$ where A, B, and C are all ordinary mesons thus consists of an integral over the product of (1) the amplitude to find the initial quark and antiquark with separation $\mathbf{r}_A$ and spins s_A and $\bar{s}_A$, (2) the amplitude for the ground-state string of meson A to break at various points $\frac{1}{2}\mathbf{r}_A + \mathbf{y}$ into two other ground-state strings with equilibrium positions along the vectors $\mathbf{r}_B$ and $\mathbf{r}_C$ [see Fig. 4(a)], and (3) the amplitude to find the

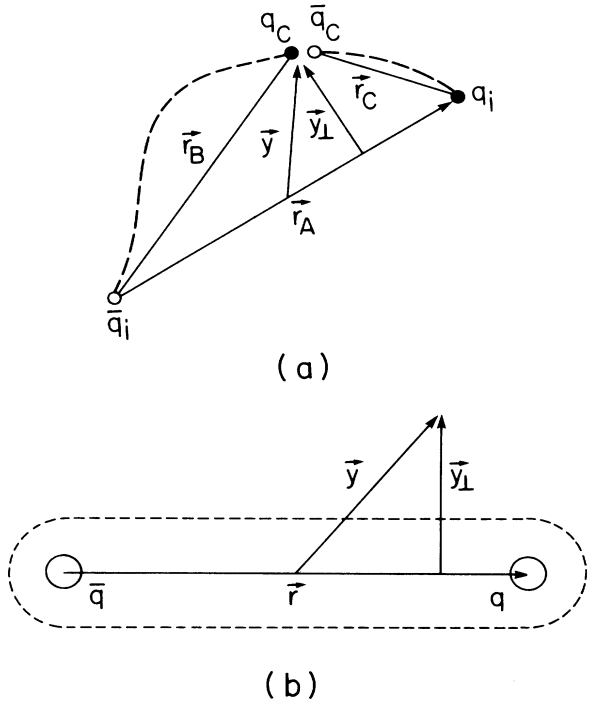

FIG. 4. (a) $A \to BC$ by flux-tube breaking at the point $\mathbf{r}/2 + \mathbf{y}$, (b) a contour of $\gamma_{00}^0(\mathbf{n})$.

new quark and antiquark, produced by Eq. (3), and the old $q\bar{q}$ pair in the wave functions of their respective mesons B and C, with relative coordinates $\mathbf{r}_B$ and $\mathbf{r}_C$ and spins s_B, $\bar{s}_B$ and s_C, $\bar{s}_C$. That is, in the rest frame of A, for equal-mass quarks,

$$M(A\to BC)=\int d^3\mathbf{r}\int d^3\mathbf{y}\,\psi_B^*\left[\frac{\mathbf{r}}{2}+\mathbf{y}\right]\psi_C^*\left[\frac{\mathbf{r}}{2}-\mathbf{y}\right]$$
$$\times\boldsymbol{\alpha}\cdot(i\overleftarrow{\nabla}_B+i\overleftarrow{\nabla}_C+\mathbf{q})$$
$$\times\psi_A(\mathbf{r})e^{i\mathbf{q}\cdot\mathbf{r}/2}\gamma_{00}^0(\mathbf{r},\mathbf{y})\,, \qquad (6)$$

where $\mathbf{q}$ is the momentum of B. (In the unequal-mass case this formula is modified; see Appendix B.)

To extract predictions from the model, it must be combined with a set of wave functions for the mesons A, B, and C. We have examined two different choices for such wave functions: (i) the exact wave functions from a recent study of mesons in a relativized version of the QCD-improved quark model[8] and (ii) a set of harmonic-oscillator wave functions characterized by a harmonic-oscillator parameter β [i.e., $\psi\sim$ (polynomial factor) $\times\exp(-\frac{1}{2}\beta^2r^2)$]. In each case the constant γ_0 of (5) was taken to be a free parameter. In case (i) this was the *only* parameter of the decay analysis; in case (ii), β was an additional parameter. The less realistic and less predictive harmonic-oscillator wave functions were examined both to check the sensitivity of our results and since in the limit $\gamma_{00}^0(\mathbf{n})=$const they allowed us to perform integrations exactly. The analytic forms thereby obtained reveal the relationships which exist between amplitudes and also allow us to make a connection in this limit to the standard $^3P_0$ pair-creation model. [Note that while within our context β is an additional parameter, this point of view is somewhat artificial. In practice β is rather well constrained by requiring it to correspond to a reasonable dynamic model for the mesons. Indeed, as will be seen below (e.g., in Table I) the fitted parameter β has a value which corresponds to a set of meson wave functions which are very similar to those of case (i).]

The more fundamental wave functions of case (i) from Ref. 8 are based on a constituent-quark model with dynamics suggested by QCD (including a linear confining potential, a Coulombic potential with a running coupling constant, and the various short-range spin-dependent interactions expected as corrections to these static potentials) in which various relativistic effects were taken into account (including relativistic kinematics, quark smearing effects, and relativistic modifications of the interquark potentials). The model, which was applied to all mesons from $u\bar{u}$ to $b\bar{b}$, gives not only a reasonable spectroscopy of mesons, but is also capable of explaining many of their characteristics, including static properties and electromagnetic and weak decay amplitudes. The authors of Ref. 8 also subjected their model to a strong decay analysis based on the pointlike meson emission model mentioned earlier, but this test, while successful, was weakened by the limitation to pseudoscalar emission and by the introduction of a necessary but unsatisfactorily large number of decay amplitudes. Our more fundamental single-parameter analysis is in good agreement with their multiparameter fit and thus lends support to their claim to have produced a reasonable set of meson wave functions and masses. On the other hand, our experience with the less realistic harmonic-oscillator wave functions indicates to us that the *main systematics* of meson decays can be understood in terms of a string-breaking picture based on any constituent-quark model in which the wave functions develop sizes, radial nodes, and orbital r^lY_{lm} factors expected for a confined $q\bar{q}$ pair.

TABLE I. Meson effective β values (GeV). The "effective β" of a state is defined to be the β of the corresponding harmonic-oscillator wave function which reproduces that state's rms momentum. (See Appendix B.)

Sector	$I=1$	$I=0$ $u\bar{u}, d\bar{d}$	$I=0$ $s\bar{s}$	Strange $u\bar{s}$	Charmed $c\bar{u}$
$1\,^1S_0$	0.75	0.75	0.73	0.71	0.66
$2\,^1S_0$	0.45	0.45	0.46	0.44	
$1\,^3S_1$	0.45	0.45	0.51	0.48	0.54
$2\,^3S_1$	0.40	0.40	0.43	0.41	
$1\,^1P_1$	0.44	0.44	0.46	0.45	0.50
$2\,^1P_1$	0.40	0.40	0.41	0.40	
$1\,^3P_0$	0.50	0.50	0.52	0.50	0.54
$2\,^3P_0$	0.41	0.41	0.42	0.41	
$1\,^3P_1$	0.44	0.44	0.47	0.45	0.50
$2\,^3P_1$	0.39	0.39	0.41	0.40	
$1\,^3P_2$	0.37	0.37	0.41	0.39	0.45
$2\,^3P_2$	0.36	0.36	0.39	0.37	
$1\,^1D_2$	0.38	0.38	0.40	0.39	
$1\,^3D_1$	0.42	0.42	0.44	0.42	
$1\,^3D_2$	0.38	0.38	0.41	0.39	
$1\,^3D_3$	0.34	0.34	0.38	0.36	
$1\,^3F_4$	0.33	0.33	0.35	0.34	

III. RESULTS

Table II shows the main results of this paper. We have tabulated here not only all known decays of normal $q\bar{q}$ mesons, but also many decays which are of possible interest in future searches for "missing" mesons. We have shown signed amplitudes (which when squared give directly the decay partial widths in MeV) so that comparison can also be made to signs when they are measured. We quote our results in the LS basis; the factors for converting the helicity amplitudes obtainable directly from (6) to this basis and our treatment of phase space are discussed in Appendixes C and D. In column (4) of Table II, next to the experimental data in column (5), we show our result for the flux-tube-breaking model with case (i) wave functions. In column (1) we give, when it is available (some calculations were done only by numerical integration), the analytic expression for the decay amplitude in the limit of a constant $\gamma_{00}^{0}(\mathbf{n})$ (i.e., the usual $^3P_0$ model) for the case (ii) (harmonic-oscillator) wave functions; in column (2) we give the corresponding numerical amplitudes (with $\beta=0.40$ GeV). In column (3) we show the results of the flux-tube model for case (ii) wave functions (once again with $\beta=0.40$ GeV). We have checked[6] that the use of the more realistic case (i) wave functions of Ref. 8 produces changes in column (2) similar to those that can be seen between columns (3) and (4). The "effective β" values for the Ref. 8 wave functions, obtained by fitting to their rms momenta, are give in Table I. In every case we have fitted the pair-creation constant γ_0 of (5) to $\rho\to\pi\pi$: for columns (2), (3), and (4) we find the values $\gamma_0=0.39$, 0.64, and 0.78 respectively.

One of the most striking features of the results of Table II is that in a very wide range of circumstances our flux-tube-breaking model gives results which are very similar to the naive quark-pair-creation model [compare columns (2) and (3) which both use case (ii) wave functions]. Given that this latter model creates quark pairs with an equal amplitude throughout space instead of within the flux tube, we at first found this correspondence surprising, but it has a simple explanation: the naive pair-creation model "accidentally" imposes a flux-tube-like structure. This fortuitous situation arises via the meson-wave-function overlap integrals which automatically diminish the importance of a pair created far from the line between the original quark and antiquark: the newly created quark and antiquark of such a pair are unlikely to overlap well with their new antiquark and quark partners.

This correspondence will obviously not be complete, but its approximate validity for relatively low-lying states offers a satisfying explanation for the remarkable success[5] of the naive quark-pair-creation model. We consider the demonstration of a probable connection between this useful old model and QCD to be one of the important results of this work.

In this regard, we now return to the question of averaging Eq. (2) over orientations of $\hat{\mathbf{e}}$ to arrive at Eq. (3). If this averaging were incomplete, one would expect both a residual of the first term in (2) and also a nonsphericity in its second term. A surviving component of the $q^{\dagger}\alpha\cdot\hat{\mathbf{e}}q$ term would create the $q\bar{q}$ pair in a state of $S=1$ with spin projection zero along the original meson axis. Pair creation in this state alone is not allowed by the data: for example, it would give

$$\Gamma(\rho\to\pi\pi):\Gamma[B\to(\omega\pi)_S]\simeq 1:30\ ,$$

very far from the experimental ratio of 1:1, and a D:S amplitude ratio in $B\to\omega\pi$ of 0.05, very far from the experimental ratio of 0.29 ± 0.05. Thus any significant admixture of such an operator is ruled out. Figure 5 shows a fit of various prominent decay modes to a pair-creation operator of the form

$$Y_{11}\chi_{1-1}+Y_{1-1}\chi_{11}-\alpha Y_{10}\chi_{10}$$

(Y_{lm} and χ_{sm} are the orbital and spin wave functions of the produced $q\bar{q}$ pair) showing also that there is no significant deviation from sphericity in the average of the second term in column (2): ignoring systematic errors, this fit gives $\alpha=0.92\pm0.02$.

Before proceeding to more specific topics for discussion in the next sections, we also briefly comment on one other general feature of this analysis. Recall that the derivation of Eq. (3) did not produce any explicit SU(3) breaking in the pair-creation amplitude. As can be seen from our results for such ratios as $A_2\to K\bar{K}/A_2\to\rho\pi$ and $f\to K\bar{K}/f=\pi\pi$, no such SU(3) breaking is required. Within the accuracy of the model, the observed departures from SU(3) can all be attributed to differences in phase space and to a wave-function-overlap effect: heavy quarks produced by string breaking are less likely to find themselves in the smaller wave functions of the resulting final-state mesons. (This is equivalent to the statement that heavier quarks, after being produced, must tunnel further to compensate for the extra string energy their massiveness consumes.) We consider this explanation of SU(3) breaking another of the important results of this work, even though the precision of this statement is compromised by the phase-space ambiguities discussed in Appendix D.

While we believe these general characteristics of our model are important, we consider the agreement that our very large body of tabulated amplitudes achieves with known meson decay rates our most significant result. Of course the model's predictive ability is limited: this is evident in both small but significant discrepancies with experiment and in the presently unavoidable dependence of its predictions on meson wave functions [compare columns (3) and (4)]. Our predictions are also dependent on relativistic effects (including ambiguities associated with relativistic phase space). Indeed, there is a certain lack of consistency in using the "relativized" wave functions of Ref. 8 with our nonrelativistic formula Eq. (6); this may account for the fact that the case (i) wave functions do somewhat worse in describing decays to pseudoscalar-meson final states (these being the most relativistic states of the Ref. 8 phenomenology). We therefore prefer to view the results of columns (3) and (4) together and to consider a discrepancy between them as indicative of the inherent uncertainty of our predictions.

Despite these shortcomings, we believe there is little doubt that the model can predict with impressive reliability the main features of meson decays. This gives us confi-

TABLE II. Meson decay amplitudes. The signed amplitudes of columns (2), (3), (4), and (5) are defined so that their squares give predicted or observed partial widths to the indicated channel. The amplitude formulas of column (1), as defined in Appendix B, do not include various phase-space factors [see Eq. (D1)]. Our notation (which we suppress when only one channel is available) is $A\to(BC)_{L,S}$ where $L=S,P,D,\ldots$ is the relative orbital angular momentum of B and C and S is their total spin. We denote by π, η, η', K, ρ, ω, ϕ, K^* the usual ground-state ($^1S_0$ and $^3S_1$) mesons; our names for other states are defined by the table subheadings below [note, e.g., that δ_2 is the broad $I=1$, $1\,^3P_0$ $q\bar{q}$ meson of Ref. 8 and not the $\delta(980)$]. The results in column (1) are for ideally mixed isoscalars except for the ground-state pseudoscalars, where we quote results for $\eta=(1/\sqrt{2})[(1/\sqrt{2})(u\bar{u}+d\bar{d})-s\bar{s}]$ and $\eta'=(1/\sqrt{2})[(1/\sqrt{2})(u\bar{u}+d\bar{d})+s\bar{s}]$; numerical results are for initial mesons with the isoscalar mixtures calculated in Ref. 8. Note that a factor of $+i$ has been suppressed in all odd partial waves. See Appendix D for the treatment of channels which are nominally below threshold; when relevant, we show the actual final-state particles of a decay in the notation $A\to(XY)_BC$, where B is a broad resonance decaying to XY. [The formulas in column (1) are in the narrow-resonance approximation and so apply to the sum of all $B\to XY$ final states.] We use experimental masses for the mesons when known; otherwise we use the masses of Ref. 8 (given below in parentheses after the particle names).

Decay	(1) Amplitude	(2) γ_{00}^0=const [Case (ii)]	(3) Flux tube [Case (ii)]	(4) Flux tube [Case (i)]	(5) Experiment[a]	(6) Comments
$1\,^3S_1$: $J^{PC}{}_n=1^{--}$						
$\rho\to\pi\pi$	$\sqrt{3}P_1$	$+12.4$	$+12.4$	$+12.4$	$+12.4$	Fit
$\phi\to K\bar{K}$	$-\sqrt{3}P_1$	-2.6	-2.6	-2.5	1.9 ± 0.1	
$K^*\to K\pi$	$\frac{3}{2}P_1$	$+7.9$	$+7.9$	$+7.8$	7.1 ± 0.1	
$1\,^3P_2$: $J^{PC}{}_n=2^{++}$						
$A_2\to(\pi\pi)_\rho\pi$	$-\sqrt{3}D_1$	-6.5	-6.7	-7.9	8.8 ± 0.3	
$A_2\to\eta\pi$	$(\frac{1}{2})^{1/2}D_1$	$+4.8$	$+4.9$	$+4.1$	4.0 ± 0.1	
$A_2\to K\bar{K}$	$-(\frac{1}{2})^{1/2}D_1$	-3.3	-3.4	-2.8	2.3 ± 0.1	
$A_2\to\eta'\pi$	$-(\frac{1}{2})^{1/2}D_1$	$+1.2$	$+1.2$	$+0.8$	<1.5	
$f\to\pi\pi$	$-(\frac{3}{2})^{1/2}D_1$	-11	-11	-8.9	12 ± 1	
$f\to K\bar{K}$	$-(\frac{1}{2})^{1/2}D_1$	-3.1	-3.1	-2.7	2.3 ± 0.2	
$f\to\eta\eta$	$(\frac{1}{8})^{1/2}D_1$	$+1.0$	$+1.0$	$+0.9$	1.0 ± 0.2[b]	
$f'\to\pi\pi$	0	$+1.0$	$+0.9$	$+0.8$	0.8 ± 0.4	
$f'\to K\bar{K}$	$-D_1$	-7.7	-7.8	-6.5	$\leq 8\pm1$	
$f'\to\eta\eta$	$\frac{1}{2}D_1$	$+3.2$	$+3.2$	$+2.5$	<6	
$f'\to\eta'\eta$	$-(\frac{1}{2})^{1/2}D_1$	-0.3	-0.3	-0.2		
$f'\to(K\pi)_{K^*}\bar{K}$	$(\frac{3}{2})^{1/2}D_1$	$+2.6$	$+2.1$	$+2.1$	<5	c
This state can also decay via $\rho\rho,\omega\omega$						
$K^*\to K\pi$	$(\frac{3}{4})^{1/2}D_1$	$+7.6$	$+7.8$	$+6.5$	6.7 ± 0.5	
$K^*\to(K\pi)_{K^*}\pi$	$-(\frac{9}{8})^{1/2}D_1$	-3.9	-4.1	-4.1	5.0 ± 0.5	
$K^*\to(\pi\pi)_\rho K$	$-(\frac{9}{8})^{1/2}D_1$	-3.0	-3.3	-3.4	3.0 ± 0.4	
$K^*\to\omega K$	$(\frac{3}{8})^{1/2}D_1$	$+1.2$	$+1.3$	$+1.4$	2.0 ± 0.4	
$K^*\to K\eta$	$\frac{1-\sqrt{2}}{\sqrt{8}}D_1$	-0.8	-0.8	-0.7	$2.2_{-2.2}{}^{+1.1}$	
$K^*\to K\eta'$	$\frac{1+\sqrt{2}}{\sqrt{8}}D_1$	$+0.2$	$+0.2$[d]	$+0.2$[d]		
$K^*\to(K\pi)_{K^*}\eta$	$-\frac{\sqrt{3}(1+\sqrt{2})}{4}D_1$	-0.6	-0.6[d]	-0.6[d]		
This state can also decay via $Q_1\pi$						
$1\,^3P_1$: $J^{PC}{}_n=1^{++}$						
$A_1\to[(\pi\pi)_\rho\pi]_S$	$\sqrt{32}S_1$	$+19$	$+20$	$+26$	18 ± 2	
$A_1\to[(\pi\pi)]_\rho\pi]_D$	$-D_1$	-5.0	-5.1	-5.0		

TABLE II. (*Continued*).

Decay	(1) Amplitude	(2) γ_{00}^0=const [Case (ii)]	(3) Flux tube [Case (ii)]	(4) Flux tube [Case (i)]	(5) Experiment[a]	(6) Comments
$A_1 \to (\pi\pi)_\epsilon \pi$	$-(\frac{8}{9})^{1/2} P_2$	−4.0	−4.0[d]	−4.0[d]		
$A_1 \to (K\bar{K})_\epsilon \pi$		−0.7	−0.7[d]	−0.7[d]		
$D \to (\eta\pi)_{\delta_2} \pi$	$(\frac{8}{3})^{1/2} P_2$	+3.1	+3.1[d]	+3.1[d]	Total width to $\eta\pi\pi$ 13±3 MeV	e
$D \to (\pi\pi)_\epsilon \eta$	$-\frac{2}{3} P_2$	−1.8	−1.8[d]	−1.8[d]		e
$D \to [(K\pi)_{K^*} \bar{K}]_S$	$\sqrt{8} S_1$	+1.2	+1.2[d]	+1.2[d]	Total width to $K\bar{K}\pi$= 3±1 MeV	e,c
$D \to [(K\pi)_{K^*} \bar{K}]_D$	$-\frac{1}{2} D_1$	+0.06	+0.06[d]	+0.06[d]		e,c
$D \to (K\bar{K})_{\delta_2} \pi$	$(\frac{8}{3})^{1/2} P_2$	+0.9	+0.9[d]	+0.9[d]		e
$D \to (\eta'\pi)_{\delta_2} \pi$	$(\frac{8}{3})^{1/2} P_2$	+0.1	+0.1[d]	+0.1[d]		e
This state can also decay via $A_1\pi$						
$E \to [(K\pi)_{K^*} \bar{K}]_S$	$-4S_1$	−11	−12	−15	f	e,c
$E \to [(K\pi)_{K^*} \bar{K}]_D$	$(\frac{1}{2})^{1/2} D_1$	+0.7	+0.7	+0.7	f	e,c
$E \to (\eta\pi)_{\delta_2} \pi$	0	≈0	≈0	≈0	f	e
$E \to (K\bar{K})_{\delta_2} \pi$		≈0	≈0	≈0	f	e
$E \to (K\bar{K})_{\epsilon_s} \eta$	$-(\frac{8}{9})^{1/2} P_2$	≈0	≈0	≈0	f	e
This state can also decay via $A_1\pi$						
$1\,^3P_1$ and $1\,^1P_1$ (strange)[g]: $J^P = 1^+$						
$Q_1 \to [(K\pi)_{K^*} \pi]_S$	$-\sqrt{6} S_1$	+1.0	+1.1	+1.4	2.7±1.5[h]	
$Q_1 \to [(K\pi)_{K^*} \pi]_D$	$-(\frac{3}{4})^{1/2} D_1$	−2.7	−2.7	−2.5	2.6±0.5[h]	
$Q_1 \to [(\pi\pi)_\rho K]_S$	$\sqrt{6} S_1$	+7.9	+8.1	+10	6.2±1.0[h]	
$Q_1 \to [(\pi\pi)_\rho K]_D$	$(\frac{3}{4})^{1/2} D_1$	−0.4	−0.4	−0.4	Not seen[h]	
$Q_1 \to [\omega K]_S$	$-\sqrt{2} S_1$	−4.0	−4.0[d]	−4.0[d]	3.1±0.5[h]	
$Q_1 \to [\omega K]_D$	$-\frac{1}{2} D_1$	+0.04	+0.04[d]	+0.04[d]	Not seen[h]	
$Q_1 \to (K\pi)_\kappa \pi$	$-(\frac{4}{3})^{1/2} P_3$	−1.3	−1.3[d]	−1.3[d]	5.1±0.5	
$Q_1 \to (K\eta)_\kappa \pi$		−0.04	−0.04[d]	−0.04[d]		
$Q_1 \to (\pi\pi)_\epsilon K$	$+\frac{2}{3} P_3$	−0.2	−0.2[d]	−0.2[d]	1.6±0.4	
$Q_1 \to (K\bar{K})_\epsilon K$		≈0	≈0	≈0		
$Q_2 \to [(K\pi)_{K^*} \pi]_S$	$\sqrt{12} S_1$	+15	+15	+21	13±3	
$Q_2 \to [(K\pi)_{K^*} \pi]_D$	$-(\frac{3}{8})^{1/2} D_1$	+1.1	+1.1	+1.0	2.6±0.9	
$Q_2 \to [(\pi\pi)_\rho K]_S$	$\sqrt{12} S_1$	+1.2	+1.2	+1.6	2±2[h]	
$Q_2 \to [(\pi\pi)_\rho K]_D$	$-(\frac{3}{8})^{1/2} D_1$	−3.8	−4.2	−3.7	Not seen[h]	
$Q_2 \to [\omega K]_S$	$-2S_1$	−0.8	−0.8	−1.0	1±1[h]	
$Q_2 \to [\omega K]_D$	$(\frac{1}{8})^{1/2} D_1$	+1.6	+1.8	+1.6	Not seen[h]	
$Q_2 \to (K\pi)_\kappa \pi$	$-(\frac{2}{3})^{1/2} P_2$	−0.7	−0.7[d]	−0.7[d]	≈0	
$Q_2 \to (K\eta)_\kappa \pi$		−0.1	−0.1[d]	−0.1[d]	≈0	
$Q_2 \to (\pi\pi)_\epsilon K$	$-(\frac{2}{9})^{1/2} P_2$	−2.4	−2.4[d]	−2.4[d]	2±2[h]	
$Q_2 \to (K\bar{K})_\epsilon K$		−0.04	−0.04[d]	−0.04[d]		
This state can also decay via $Q_1\pi$						

TABLE II. (*Continued*).

Decay	(1) Amplitude	(2) γ^0_{00}=const [Case (ii)]	(3) Flux tube [Case (ii)]	(4) Flux tube [Case (i)]	(5) Experiment[a]	(6) Comments
$1\,^1P_1$: $J^{PC_n}=1^{+-}$						
$B\to[\omega\pi]_S$	$-\sqrt{8}S_1$	-11	-11	-14	12 ± 1	
$B\to[\omega\pi]_D$	$-D_1$	-2.3	-2.4	-2.5	3.6 ± 0.5	$D/S=+0.29\pm.05$
$B\to(\eta\pi)_{\delta_2}\pi$	$(\frac{32}{9})^{1/2}P_3$	$+1.2$	$+1.2$[d]	$+1.2$[d]		
$B\to(K\bar{K})_{\delta_2}\pi$		$+0.2$	$+0.2$[d]	$+0.2$[d]		
$B\to(\eta'\pi)_{\delta_2}\pi$		$+0.03$	$+0.03$[d]	$+0.03$[d]		
$H\to[(\pi\pi)_\rho\pi]_S$	$\sqrt{24}S_1$	$+15$	$+16$	$+21$	Total width= 320 ± 50 MeV	
$H\to[(\pi\pi)_\rho\pi]_D$	$\sqrt{3}D_1$	$+6.6$	$+6.7$	$+6.5$		
$H\to\epsilon\eta$	$-(\frac{8}{9})^{1/2}P_3$	-1.0	-1.0[d]	-1.0[d]		
$H'(1470)\to[(\pi\pi)_\rho\pi]_S$	0	≈0	≈0	≈0		
$H'(1470)\to[(\pi\pi)_\rho\pi]_D$	0	≈0	≈0	≈0		
$H'(1470)\to[(K\pi)_{K^*}\bar{K}]_S$	$\sqrt{8}S_1$	$+9.4$	$+9.9$	$+13$		c
$H'(1470)\to[(K\pi)_{K^*}\bar{K}]_D$	D_1	$+1.8$	$+2.2$	$+2.1$		c
$H'(1470)\to\kappa\bar{K}$	$-\frac{4}{3}P_3$	-0.8	-0.8[d]	-0.8[d]		c
$1\,^3P_0$: $J^{PC_n}=0^{++}$						
$\delta_2(1090)\to\eta\pi$	$2S_1$	$+14$	$+14$	$+21$	See IV D	
$\delta_2(1090)\to K\bar{K}$	$-2S_1$	-12	-13	-17	See IV D	
$\delta_2(1090)\to\eta'\pi$	$2S_1$	$+8.0$	$+8.0$[d]	$+8.0$[d]	See IV D	
$\epsilon(1090)\to\pi\pi$	$-\sqrt{12}S_1$	-20	-20	-36	See IV D	
$\epsilon(1090)\to K\bar{K}$	$-2S_1$	-11	-12	-15	See IV D	
$\epsilon(1090)\to\eta\eta$	S_1	$+4.2$	$+4.2$[d]	$+4.2$[d]	See IV D	
$\epsilon_s(1360)\to\pi\pi$	0	≈0	≈0	≈0	See IV D	e
$\epsilon_s(1360)\to K\bar{K}$	$-\sqrt{8}S_1$	-19	-19	-31	See IV D	
$\epsilon_s(1360)\to\eta\eta$	$\sqrt{2}S_1$	$+9.2$	$+9.4$	$+14$	See IV D	
$\kappa(1240)\to K\pi$	$\sqrt{6}S_1$	$+13$	$+13$	$+23$	See IV D	
$\kappa(1240)\to K\eta$	$(1-\sqrt{2})S_1$	-2.9	-2.9	-4.5	See IV D	
$\kappa(1240)\to K\eta'$	$(1+\sqrt{2})S_1$	≈0	≈0	≈0	See IV D	
$2\,^1S_0$: $J^{PC_n}=0^{-+}$						
$\pi_r(1300)\to(\pi\pi)_\rho\pi$	$-3P_4$	-13	-14	-21	15 ± 5	
$\pi_r(1300)\to(K\pi)_{K^*}\bar{K}$	$-\frac{3}{2}P_4$	-2.7	-2.7[d]	-2.7[d]		c
This state can also decay via $\epsilon\pi$						
$\eta_r(1440)\to(K\pi)_{K^*}\bar{K}$	$-\frac{3}{2}P_4$	-3.4	-3.5	-4.6		c
This state can also decay via $\delta_2\pi$						
$\eta'_r(1630)\to(K\pi)_{K^*}\bar{K}$	$(\frac{9}{2})^{1/2}P_4$	$+11$	$+12$	$+18$		c
This state can also decay via $\delta_2\pi,\omega\omega,\rho\rho,\epsilon\eta,\kappa\bar{K}$						
$K_r(1450)\to(K\pi)_{K^*}\pi$	$-(\frac{27}{8})^{1/2}P_4$	-9.2	-10	-14	10 ± 2	
$K_r(1450)\to(K\pi)_{K^*}\eta$	$-\frac{3(1+\sqrt{2})}{4}P_4$	-4.1	-4.5	-5.3		

TABLE II. (*Continued*).

Decay	(1) Amplitude	(2) γ^0_{00}=const [Case (ii)]	(3) Flux tube [Case (ii)]	(4) Flux tube [Case (i)]	(5) Experiment[a]	(6) Comments
$K_r(1450)\to(\pi\pi)_\rho K$	$-(\frac{27}{8})^{1/2}P_4$	−7.2	−7.7	−11	6±1	
$K_r(1450)\to\omega K$	$(\frac{9}{8})^{1/2}P_4$	+4.5	+4.8	+6.6		
$K_r(1450)\to\phi K$	$-\frac{3}{2}P_4$	−2.1	−2.1[d]	−2.1[d]		
This state can also decay via $\kappa\pi$						
$2\,^3S_1$: $J^{PC}{}_n=1^{--}$						
$\rho_r(1450)\to\pi\pi$	$(\frac{9}{2})^{1/2}P_4$	+7.1	+7.8	+3.5	See IV B	
$\rho_r(1450)\to\omega\pi$	$-3P_4$	−9.2	−9.2	−8.4	See IV B	
$\rho_r(1450)\to(\pi\pi)_\rho\eta$	$-(\frac{9}{2})^{1/2}P_4$	−4.0	−4.3	−4.0	See IV B	
$\rho_r(1450)\to K\bar{K}$	$\frac{3}{2}P_4$	+5.6	+6.0	+3.3	See IV B	
$\rho_r(1450)\to(K\pi)_{K^*}\bar{K}$	$(\frac{9}{2})^{1/2}P_4$	+1.4	+1.5	+1.3	See IV B	c
$\rho_r(1450)\to(\pi\pi)_\epsilon\rho$	$6S_2$	−0.7	−0.7[d]	−0.7[d]	See IV B	
$\rho_r(1450)\to([(\pi\pi)_\rho\pi]_S)_H\pi$	$-\sqrt{12}S_2$	−0.7	−0.7[d]	−0.7[d]	See IV B	
$\rho_r(1450)\to([(\pi\pi)_\rho\pi]_D)_H\pi$		−0.2	−0.2[d]	−0.2[d]	See IV B	
$\rho_r(1450)\to([(\pi\pi)_\rho\pi]_S)_{A_1}\pi$	$\sqrt{48}S_2$	+1.2	+1.2[d]	+1.2[d]	See IV B	
$\rho_r(1450)\to([(\pi\pi)_\rho\pi]_D)_{A_1}\pi$		+0.2	+0.2[d]	+0.2[d]	See IV B	
$\rho_r(1450)\to(\epsilon\pi)_{A_1}\pi$		−0.06	−0.06[d]	−0.06[d]	See IV B	
$\rho_r(1450)\to[(\pi\pi)_\rho(\pi\pi)_\rho]_{P,2}$		+4.2	+4.2[d]	+4.2[d]	See IV B	
$\rho_r(1450)\to[(\pi\pi)_\rho(\pi\pi)_\rho]_{F,2}$	0	0	0	0	See IV B	i
$\rho_r(1450)\to[(\pi\pi)_\rho(\pi\pi)_\rho]_{P,0}$		−8.8	−8.8[d]	−8.8[d]	See IV B	
This state can also decay via $A_2\pi,\pi_r\pi$						
$\omega_r(1460)\to(\pi\pi)_\rho\pi$	$\sqrt{27}P_4$	+16	+17	+15	See IV B	
$\omega_r(1460)\to\omega\eta$	$-(\frac{9}{2})^{1/2}P_4$	−5.0	−5.4	−5.0	See IV B	
$\omega_r(1460)\to\omega\eta'$	$-(\frac{9}{2})^{1/2}P_4$	−0.8	−0.8[d]	−0.8[d]	See IV B	
$\omega_r(1460)\to K\bar{K}$	$\frac{3}{2}P_4$	+6.1	+6.7	+3.5	See IV B	
$\omega_r(1460)\to(K\pi)_{K^*}\bar{K}$	$(\frac{9}{2})^{1/2}P_4$	+4.3	+4.6	+4.0	See IV B	c
$\omega_r(1460)\to(\pi\pi)_\epsilon\omega$	$6S_2$	+0.8	+0.8[d]	+0.8[d]	See IV B	
$\omega_r(1460)\to(K\bar{K})_\epsilon\omega$		+0.04	+0.04[d]	+0.04[d]	See IV B	
$\omega_r(1460)\to B\pi$	$6S_2$	+1.5	+1.5[d]	+1.5[d]	See IV B	
This state can also decay via $H\eta,\phi\eta$						
$\phi_r(1690)\to\phi\eta$	$3P_4$	+6.7	+7.3	+6.7	See IV B	
$\phi_r(1690)\to K\bar{K}$	$-(\frac{9}{2})^{1/2}P_4$	−8.4	−9.1	−7.7	See IV B	
$\phi_r(1690)\to(K\pi)_{K^*}\bar{K}$	$3P_4$	+9.4	+10	+11	See IV B	c
This state can also decay via $\rho\pi,\omega\eta'$						
$K_r^*(1580)\to K\pi$	$(\frac{27}{8})^{1/2}P_4$	+7.1	+7.7	+4.9	See IV B	
$K_r^*(1580)\to K\eta$	$\frac{3(1+\sqrt{2})}{4}P_4$	+7.5	+8.3	+5.2	See IV B	
$K_r^*(1580)\to K\eta'$	$-\frac{3(-1+\sqrt{2})}{4}P_4$	−0.7	−0.9	−0.5	See IV B	
$K_r^*(1580)\to(\pi\pi)_\rho K$	$(\frac{27}{4})^{1/2}P_4$	+7.4	+8.1	+8.3	See IV B	

TABLE II. (*Continued*).

Decay	(1) Amplitude	(2) γ^0_{00}=const [Case (ii)]	(3) Flux tube [Case (ii)]	(4) Flux tube [Case (i)]	(5) Experiment[a]	(6) Comments
$K_r^*(1580)\to\omega K$	$-\frac{3}{2}P_4$	−4.9	−5.3	−5.4	See IV B	
$K_r^*(1580)\to\phi K$	$-(\frac{9}{2})^{1/2}P_4$	−4.3	−4.6	−4.0	See IV B	
$K_r^*(1580)\to(K\pi)_{K^*}\pi$	$-(\frac{27}{4})^{1/2}P_4$	−8.8	−9.4	−9.1	See IV B	
$K_r^*(1580)\to(K\pi)_{K^*}\eta$	$-\frac{3(1-\sqrt{2})}{\sqrt{8}}P_4$	+1.0	+1.2	+0.9	See IV B	
$K_r^*(1580)\to Q_1\pi$	$-3S_2$	+0.3	+0.3[d]	+0.3[d]	See IV B	j,g
$K_r^*(1580)\to Q_2\pi$	$\sqrt{18}S_2$	+1.7	+1.7[d]	+1.7[d]	See IV B	i,j
This state can also decay via $K^*(1420)\pi, K_r(1450)\pi$						
$1\,^3D_3$: $J^{PC_n}=3^{--}$						
$g\to\pi\pi$	$-(\frac{3}{20})^{1/2}F_1$	−6.2	−6.4	−4.6	6.9±0.6	
$g\to\pi_r\pi$		+0.6	+0.8	+0.9		j
$g\to\omega\pi$	$(\frac{1}{5})^{1/2}F_1$	+3.7	+3.8	+3.9	5.6±1.6	
$g\to\omega_r\pi$		−0.06	−0.06	−0.09		j
$g\to K\bar{K}$	$-(\frac{3}{40})^{1/2}F_1$	−3.0	−3.2	−2.3	1.7±0.3	
$g\to(K\pi)_{K^*}\bar{K}$	$-(\frac{1}{10})^{1/2}F_1$	−1.3	−1.3	−1.3	<2.6	c
$g\to(\pi\pi)_\rho\eta$	$-(\frac{3}{20})^{1/2}F_1$	−1.9	−1.9	−2.0		
$g\to[(\pi\pi)_\rho(\pi\pi)_\rho]_{P,2}$		+4.4	+4.6	+6.0	Total width to $\rho\rho$= 60±35 MeV	
$g\to[(\pi\pi)_\rho(\pi\pi)_\rho]_{F,2}$		+1.9	+2.0	+3.0		
$g\to[(\pi\pi)_\rho(\pi\pi)_\rho]_{H,2}$	0	0	0	0		i
$g\to[(\pi\pi)_\rho(\pi\pi)_\rho]_{F,0}$		−0.9	−0.9	−1.7		
$g\to[H\pi]_D$	$(\frac{14}{45})^{1/2}D_2$	+3.0	+3.0[d]	+3.0[d]		
$g\to[H\pi]_G$	$-(\frac{32}{945})^{1/2}D_3$	+0.5	+0.5[d]	+0.5[d]		
This state can also decay via $A_2\pi, A_1\pi, \epsilon\rho, \delta_2\omega$						
$\omega\to(\pi\pi)_\rho\pi$	$-(\frac{3}{5})^{1/2}F_1$	−6.1	−6.2	−6.4	8±2	
$\omega\to\omega\eta$	$(\frac{1}{10})^{1/2}F_1$	+1.2	+1.2	+1.3		
$\omega\to\omega\eta'$	$(\frac{1}{10})^{1/2}F_1$	+0.03	+0.03[d]	+0.03[d]		
$\omega\to[B\pi]_D$	$-(\frac{14}{15})^{1/2}D_2$	−4.0	−4.0[d]	−4.0[d]	7±3	
$\omega\to[B\pi]_G$	$(\frac{32}{315})^{1/2}D_3$	−0.4	−0.4[d]	−0.4[d]		
$\omega\to K\bar{K}$	$-(\frac{3}{40})^{1/2}F_1$	−2.7	−2.7	−2.1		
$\omega\to(K\pi)_{K^*}\bar{K}$	$-(\frac{1}{10})^{1/2}F_1$	−1.0	−1.0	−1.0		c
This state can also decay via $\delta_2\rho, \epsilon\omega, H\eta, \phi\eta$						
$\phi\to\phi\eta$	$-(\frac{1}{5})^{1/2}F_1$	−1.5	−1.6	−1.4		
$\phi\to K\bar{K}$	$(\frac{3}{20})^{1/2}F_1$	+5.7	+5.8	+4.1	7±2	
$\phi\to(K\pi)_{K^*}\bar{K}$	$-(\frac{1}{5})^{1/2}F_1$	−3.0	−3.1	−2.9	5±2	c
$\phi\to[(K\pi)_{K^*}(K\pi)_{\bar{K}^*}]_{P,2}$		−4.6	−4.7	−6.0		
$\phi\to[(K\pi)_{K^*}(K\pi)_{\bar{K}^*}]_{F,2}$		−0.7	−0.7	−0.9		
$\phi\to[(K\pi)_{K^*}(K\pi)_{\bar{K}^*}]_{H,2}$	0	0	0	0		i
$\phi\to[(K\pi)_{K^*}(K\pi)_{\bar{K}^*}]_{F,0}$		+0.3	+0.3	+0.4		
This state can also decay via $Q_1\bar{K}, Q_2\bar{K}, \rho\pi, \omega\eta, B\pi$						

TABLE II. (*Continued*).

Decay	(1) Amplitude	(2) γ^0_{00}=const [Case (ii)]	(3) Flux tube [Case (ii)]	(4) Flux tube [Case (i)]	(5) Experiment[a]	(6) Comments
$K^* \to K\pi$	$-(\frac{9}{80})^{1/2}F_1$	-5.5	-5.7	-4.0	4.9 ± 1.0	
$K^* \to (K\pi)_{K^*}\pi$	$(\frac{3}{20})^{1/2}F_1$	$+3.3$	$+3.4$	$+3.3$	Seen	
$K^* \to (\pi\pi)_\rho K$	$-(\frac{3}{20})^{1/2}F_1$	-3.2	-3.4	-3.4	Seen	
$K^* \to \omega K$	$(\frac{1}{20})^{1/2}F_1$	$+1.6$	$+1.6$	$+1.7$	Seen	
$K^* \to K\eta$	$\frac{-3(1+\sqrt{2})}{\sqrt{480}}F_1$	-4.1	-4.3	-2.9		
$K^* \to K\eta'$	$\frac{3(-1+\sqrt{2})}{\sqrt{480}}F_1$	$+0.2$	$+0.2$	$+0.1$		
$K^* \to (K\pi)_{K^*}\eta$	$\frac{3(1-\sqrt{2})}{\sqrt{360}}F_1$	-0.2	-0.2	-0.2		
$K^* \to \phi K$	$\frac{1}{10}D$	$+1.0$	$+1.0$	$+1.0$		
$K^* \to [(K\pi)_{K^*}(\pi\pi)_\rho]_{P,2}$		$+3.2$	$+3.2$	$+4.2$		
$K^* \to [(K\pi)_{K^*}(\pi\pi)_\rho]_{F,2}$		$+1.4$	$+1.4$	$+1.9$		
$K^* \to [(K\pi)_{K^*}(\pi\pi)_\rho]_{H,2}$	0	0	0	0		i
$K^* \to [(K\pi)_{K^*}(\pi\pi)_\rho]_{F,1}$	0	0	0	0		k
$K^* \to [(K\pi)_{K^*}(\pi\pi)_\rho]_{F,0}$		-0.7	-0.7	-1.3		
$K^* \to [(K\pi)_{K^*}\omega]_{P,2}$		$+2.9$	$+3.0$	$+3.8$		
$K^* \to [(K\pi)_{K^*}\omega]_{F,2}$		$+0.4$	$+0.4$	$+0.5$		
$K^* \to [(K\pi)_{K^*}\omega]_{H,2}$	0	0	0	0		i
$K^* \to [(K\pi)_{K^*}\omega]_{F,1}$	0	0	0	0		k
$K^* \to [(K\pi)_{K^*}\omega]_{F,0}$		-0.2	-0.2	-0.2		
$K^* \to [HK]_D$	$(\frac{7}{90})^{1/2}D_2$	$+1.2$	$+1.2^d$	$+1.2^d$		
$K^* \to [HK]_G$	$-(\frac{8}{945})^{1/2}D_3$	$+0.2$	$+0.2^d$	$+0.2^d$		
$K^* \to [(\pi\pi)_f K]_D$		-1.1	-1.1^d	-1.1^d		
$K^* \to [(K\bar{K})_f K]_D$	$-(\frac{7}{30})^{1/2}D_2$	-0.2	-0.2^d	-0.2^d		
$K^* \to [(\eta\eta)_f K]_D$		-0.04	-0.04^d	-0.04^d		
$K^* \to [(\pi\pi)_f K]_G$		-0.2	-0.2^d	-0.2^d		
$K^* \to [(K\bar{K})_f K]_G$	$(\frac{8}{315})^{1/2}D_3$	-0.01	-0.01^d	-0.01^d		
$K^* \to [(\eta\eta)_f K]_G$		-0.001	-0.001^d	-0.001^d		
$K^* \to [BK]_D$	$-(\frac{7}{30})^{1/2}D_2$	-1.4	-1.4^d	-1.4^d		
$K^* \to [BK]_G$	$(\frac{8}{315})^{1/2}D_3$	-0.2	-0.2^d	-0.2^d		
$K^* \to [([(\pi\pi)_\rho\pi]_S)_{A_1}K]_D$		-1.7	-1.7^d	-1.7^d		
$K^* \to [([(\pi\pi)_\rho\pi]_D)_{A_1}K]_D$		-0.1	-0.1^d	-0.1^d		
$K^* \to [(\epsilon\pi)_{A_1}K]_D$		-0.01	-0.01^d	-0.01^d		
$K^* \to [([(\pi\pi)_\rho\pi]_S)_{A_1}K]_G$		-0.3	-0.3^d	-0.3^d		
$K^* \to [([(\pi\pi)_\rho\pi]_D)_{A_1}K]_G$	$(\frac{8}{315})^{1/2}D_3$	-0.01	-0.01^d	-0.01^d		
$K^* \to [(\epsilon\pi)_{A_1}K]_G$		≈ 0	≈ 0	≈ 0		
This state can also decay via $Q_1\pi, Q_2\pi, K^*(1420)\pi, \epsilon K^*, \delta_2 K^*$						
$1\,^3D_2$ (nonstrange): $J^{PC_n}=2^{--}$						
$\rho(1700) \to [\omega\pi]_P$	$-(\frac{20}{3})^{1/2}P_5$	-6.2	-6.4	-7.6		
$\rho(1700) \to [\omega\pi]_F$	$(\frac{1}{10})^{1/2}F_1$	$+3.3$	$+3.3$	$+3.3$		

TABLE II. (*Continued*).

Decay	(1) Amplitude	(2) γ^0_{00}=const [Case (ii)]	(3) Flux tube [Case (ii)]	(4) Flux tube [Case (i)]	(5) Experiment[a]	(6) Comments
$\rho(1700)\to[\omega_r\pi]_P$		+3.0	+3.0	+0.3		j
$\rho(1700)\to[\omega_r\pi]_F$		−0.07	−0.07	−0.09		j
$\rho(1700)\to[(\pi\pi)_\rho\eta]_P$	$-(\frac{10}{3})^{1/2}P_5$	−3.8	−3.9	−4.4		
$\rho(1700\to[(\pi\pi)_\rho\eta]_F$	$(\frac{1}{20})^{1/2}F_1$	+1.8	+1.8	+1.8		
$\rho(1700)\to[(K\pi)_{K^*}\bar{K}]_P$	$(\frac{10}{3})^{1/2}P_5$	+4.0	+4.1	+4.8		c
$\rho(1700)\to[(K\pi)_{K^*}\bar{K}]_F$	$-(\frac{1}{20})^{1/2}F_1$	−1.3	−1.3	−1.1		c
$\rho(1700)\to[A_2\pi]_S$	$(\frac{1600}{3})^{1/2}S_3$	+16	+16[d]	+16[d]		
$\rho(1700)\to([(\pi\pi)_\rho\pi]_S)_H\pi$		−3.6	−3.6[d]	−3.6[d]		
$\rho(1700)\to([(\pi\pi)_\rho\pi]_D)_H\pi$	$-(\frac{8}{9})^{1/2}D_4$	−1.0	−1.0[d]	−1.0[d]		
$\rho(1700)\to(\epsilon\eta)_H\pi$		≈0	≈0	≈0		
$\rho(1700)\to B\eta$	$-\frac{2}{3}D_4$	1.0	1.0	1.0		
$\rho(1700)\to[(\pi\pi)_\rho(\pi\pi)_\rho]_{P,2}$		+1.9	+2.0	+2.5		
$\rho(1700)\to[(\pi\pi)_\rho(\pi\pi)_\rho]_{F,2}$	$-(\frac{7}{30})^{1/2}D_2$	+5.9	+5.9	+8.0		
This state can also decay via $(A_2\pi)_D,(A_2\pi)_G,A_1\pi,\delta_2\pi$						
$\omega(1700)\to[(\pi\pi)_\rho\pi]_P$	$\sqrt{20}P_5$	9.3	+10	+12		
$\omega(1700)\to[(\pi\pi)_\rho\pi]_F$	$-(\frac{3}{10})^{1/2}F_1$	−5.6	−5.8	−5.7		
$\omega(1700)\to[\rho_r\pi]_P$		−5.6	−5.7	−0.5		j
$\omega(1700)\to[\rho_r\pi]_F$		+0.2	+0.2	+0.2		j
$\omega(1700)\to[\omega\eta]_P$	$-(\frac{10}{3})^{1/2}P_5$	−4.4	−4.5	−5.2		
$\omega(1700)\to[\omega\eta]_F$	$(\frac{1}{20})^{1/2}F_1$	+1.2	+1.3	+1.3		
$\omega(1700)\to[(K\pi)_{K^*}\bar{K}]_P$	$(\frac{10}{3})^{1/2}P_5$	+4.1	+4.2	+4.9		c
$\omega(1700)\to[(K\pi)_{K^*}\bar{K}]_F$	$-(\frac{1}{20})^{1/2}F_1$	−1.1	−1.1	−0.9		c
$\omega(1700)\to B\pi$	$(\frac{8}{3})^{1/2}D_4$	+5.0	+5.0[d]	+5.0[d]		
This state can also decay via $H\eta,\omega\epsilon,\phi\eta$						
$\phi(1910)\to[(K\pi)_{K^*}\bar{K}]_P$	$(\frac{20}{3})^{1/2}P_5$	+6.6	+6.7	+8.3		c
$\phi(1910)\to[(K\pi)_{K^*}\bar{K}]_F$	$-(\frac{1}{10})^{1/2}F_1$	−3.1	−3.2	−2.9		c
$\phi(1910)\to[\phi\eta]_P$	$(\frac{20}{3})^{1/2}P_5$	+6.7	+6.8	+8.0		
$\phi(1910)\to[\phi\eta]_F$	$-(\frac{1}{10})^{1/2}F_1$	−1.7	−1.9	−1.5		
$\phi(1910)\to[(K\pi)_{K^*}(K\pi)_{\bar{K}^*}]_{P,2}$		−2.4	−2.5	−3.1		
$\phi(1910)\to[(K\pi)_{K^*}(K\pi)_{\bar{K}^*}]_{F,2}$		−2.8	−2.8	−3.1		
This state can also decay via $Q_1\bar{K},Q_2\bar{K},\kappa\bar{K},\phi\epsilon,\rho\pi,\omega\eta$						
1^3D_2 and 1^1D_2 (strange)[g]: $J^P=2^-$						
$L_1(1780)\to[(\pi\pi)_\rho K]_P$	$(\frac{10}{3})^{1/2}P_5$	+5.8	+6.0	+7.2		
$L_1(1780)\to[(\pi\pi)_\rho K]_F$	$(\frac{9}{80})^{1/2}F_1$	+1.2	+1.3	+1.2		
$L_1(1780)\to[\omega K]_P$	$-(\frac{10}{9})^{1/2}P_5$	−4.0	−4.1	−4.9	Seen	
$L_1(1780)\to[\omega K]_F$	$-(\frac{3}{80})^{1/2}F_1$	−0.6	−0.6	−0.6		
$L_1(1780)\to[(K\pi)_{K^*}\pi]_P$	$(\frac{10}{3})^{1/2}P_5$	+0.7	+0.7	+0.9	See L_2 listing	
$L_1(1780)\to[(K\pi)_{K^*}\pi]_F$	$(\frac{9}{80})^{1/2}F_1$	+1.4	+1.4	+1.3		

TABLE II. (*Continued*).

Decay	(1) Amplitude	(2) γ^0_{00}=const [Case (ii)]	(3) Flux tube [Case (ii)]	(4) Flux tube [Case (i)]	(5) Experiment[a]	(6) Comments
$L_1(1780)\to[(K\pi)_{K^*}\eta]_P$	$\frac{\sqrt{5}(1+\sqrt{2})}{3}P_5$	+3.9	+4.0	+4.7		
$L_1(1780)\to[(K\pi)_{K^*}\eta]_F$	$\frac{3(1+\sqrt{2})}{\sqrt{480}}F_1$	+1.3	+1.3	+1.2		
$L_1(1780)\to[\phi K]_P$	$-(\frac{20}{9})^{1/2}P_5$	−5.1	−5.2	−6.0	Seen	
$L_1(1780)\to[\phi K]_F$	$-(\frac{3}{40})^{1/2}F_1$	−0.4	−0.4	−0.3		
$L_1(1780)\to[KA_2]_S$	$-(\frac{400}{3})^{1/2}S_3$	5.9	5.9[d]	5.9[d]		
$L_1(1780)\to[Kf]_S$	$-(\frac{400}{3})^{1/2}S_3$	−8.4	−8.4[d]	−8.4[d]	6±2	
$L_1(1780)\to[K^*(1420)\pi]_S$	$(\frac{400}{3})^{1/2}S_3$	+1.5	+1.5[d]	+1.5[d]	See L_2 listing	
$L_1(1780)\to[(K\pi)_{K^*}(\pi\pi)_\rho]_{P,2}$	0	+0.2	+0.2	+0.2		k
$L_1(1780)\to[(K\pi)_{K^*}(\pi\pi)_\rho]_{F,2}$	0	+1.5	+1.5	+1.3		k
$L_1(1780)\to[(K\pi_{K^*}(\pi\pi)_\rho]_{P,1}$		+1.7	+1.7	+2.2		
$L_1(1780)\to[(K\pi)_{K^*}(\pi\pi)_\rho]_{F,1}$		+1.4	+1.4	+1.5		
$L_1(1780)\to[(K\pi)_{K^*}\omega]_{P,2}$	0	+0.7	+0.8	+0.8		k
$L_1(1780)\to[(K\pi)_{K^*}\omega]_{F,2}$	0	+0.4	+0.4	+0.3		k
$L_1(1780)\to[(K\pi)_{K^*}\omega]_{P,1}$		+1.6	+1.6	+2.0		
$L_1(1780)\to[(K\pi)_{K^*}\omega]_{F,1}$		+0.3	+0.3	+0.4		
This state can also decay via $K\epsilon,\kappa\pi,K\delta_2,KB,KA_1,KH,KD$						
$L_2(1810)\to[(\pi\pi)_\rho K]_P$	$\sqrt{5}P_5$	+2.0	+2.0	+2.4		
$L_2(1810)\to[(\pi\pi)_\rho K]_F$	$-(\frac{3}{40})^{1/2}F_1$	−4.3	−4.4	−4.2		
$L_2(1810)\to[\omega K]_P$	$-(\frac{5}{3})^{1/2}P_5$	−1.3	−1.3	−1.6	See L_1 listing	
$L_2(1810)\to[\omega K]_F$	$(\frac{1}{40})^{1/2}F_1$	+2.2	+2.3	+2.2		
$L_2(1810)\to[(K\pi)_{K^*}\pi]_P$	$-\sqrt{5}P_5$	−7.0	−7.2	−8.9	7±2	
$L_2(1810)\to[(K\pi)_{K^*}\pi]_F$	$(\frac{3}{40})^{1/2}F_1$	+0.5	+0.5	+0.4		
$L_2(1810)\to[(K\pi)_{K^*}\eta]_P$	$\frac{\sqrt{5}(-1+\sqrt{2})}{\sqrt{6}}P_5$	−1.6	−1.7	−1.9		
$L_2(1810)\to[(K\pi)_{K^*}\eta]_F$	$\frac{1-\sqrt{2}}{\sqrt{80}}F_1$	−1.4	−1.4	−1.2		
$L_2(1810)\to[\phi K]_P$	$-(\frac{10}{3})^{1/2}P_5$	−1.8	−1.8	−2.1	See L_1 listing	
$L_2(1810)\to[\phi K]_F$	$(\frac{1}{20})^{1/2}F_1$	+1.4	+1.4	+1.2		
$L_2(1810)\to[KA_2]_S$	$-10\sqrt{2}S_3$	2.6	2.6[d]	2.6[d]		
$L_2(1810)\to[Kf]_S$	$-10\sqrt{2}S_3$	−3.2	−3.2[d]	−3.2[d]	See L_1 listing	
$L_2(1810)\to[K^*(1420)\pi]_S$	$-10\sqrt{2}S_3$	−14	−14[d]	−14[d]	11±3	
$L_2(1810)\to[(K\pi)_{K^*}(\pi\pi)_\rho]_{P,2}$		+1.6	+1.7	+2.1		
$L_2(1810)\to[(K\pi)_{K^*}(\pi\pi)_\rho]_{F,2}$		+3.0	+3.3	+3.9		
$L_2(1810)\to[(K\pi)_{K^*}(\pi\pi)_\rho]_{P,1}$	0	−1.8	−1.8	−2.6		k
$L_2(1810\to[(K\pi)_{K^*}(\pi\pi)_\rho]_{F,1}$	0	−1.1	−1.1	−2.4		k
$L_2(1810)\to[(K\pi)_{K^*}\omega]_{P,2}$		+1.3	+1.3	+1.6		
$L_2(1810)\to[(K\pi)_{K^*}\omega]_{F,2}$		+0.9	+0.9	+1.0		
$L_2(1810)\to[(K\pi)_{K^*}\omega]_{P,1}$	0	−1.2	−1.2	−1.8		k
$L_2(1810)\to[(K\pi)_{K^*}\omega]_{F,1}$	0	−0.3	−0.3	−0.7		k
This state can also decay via $K\epsilon,\kappa\pi,K\delta_2,KB,KA_1,KH,KD$						

TABLE II. (*Continued*).

Decay	(1) Amplitude	(2) γ_{00}^0=const [Case (ii)]	(3) Flux tube [Case (ii)]	(4) Flux tube [Case (i)]	(5) Experiment[a]	(6) Comments
$1\,^1D_2$ (nonstrange): $J^{PC_n}=2^{-+}$						
$A_3\to[(\pi\pi)_\rho\pi]_P$	$(\frac{80}{9})^{1/2}P_5$	+6.3	+6.5	+7.7	Total width to $\rho\pi$= 85±35 MeV	
$A_3\to[(\pi\pi)_\rho\pi]_F$	$(\frac{3}{10})^{1/2}F_1$	+5.5	+5.6	+5.6		
$A_3\to[(\rho_r\pi)_P$		−2.8	−3.0	+0.3		j
$A_3\to[\rho_r\pi]_F$		−0.2	−0.2	+0.1		j
$A_3\to[(K\pi)_{K^*}\bar{K}]_P$	$(\frac{20}{9})^{1/2}P_5$	+3.3	+3.4	+4.0	2.2±0.6	c
$A_3\to[(K\pi)_{K^*}\bar{K}]_F$	$(\frac{3}{40})^{1/2}F_1$	+1.2	+1.4	+1.2		c
$A_3\to[f\pi]_S$	$-\frac{40}{3}S_3$	−9.2	−9.2[d]	−9.2[d]	11±2	
$A_3\to[D\pi]_D$	$-(\frac{2}{3})^{1/2}D_5$	−1.9	−1.9[d]	−1.9[d]		
$A_3\to[B\pi]_D$	0	0	0	0		i
$A_3\to[(\pi\pi)_\rho\omega]_{P,2}$	0	0	0	0		i
$A_3\to[(\pi\pi)_\rho\omega]_{P,1}$		−2.0	−2.1	−2.6		
$A_3\to[(\pi\pi)_\rho\omega]_{F,2}$	0	0	0	0		i
$A_3\to[(\pi\pi)_\rho\omega]_{F,1}$		−0.9	−0.9	−1.2		
This state can also decay via $\pi\epsilon,\eta\delta_2,[f\pi]_D$						
$\omega(1680)\to[(K\pi)_{K^*}\bar{K}]_P$	$(\frac{20}{9})^{1/2}P_5$	+3.4	+3.5	+4.1		c
$\omega(1680)\to[(K\pi)_{K^*}\bar{K}]_F$	$(\frac{3}{40})^{1/2}F_1$	+1.4	+1.6	+1.4		c
$\omega(1680)\to([(\pi\pi)_\rho\pi]_S)_{A_1}\pi$		+4.6	+4.6[d]	+4.6[d]		
$\omega(1680)\to([(\pi\pi)_\rho\pi]_D)_{A_1}\pi$	$\sqrt{2}D_5$	+0.7	+0.7[d]	+0.7[d]		
$\omega(1680)\to(\epsilon\pi)_{A_1}\pi$		+0.3	+0.3[d]	+0.3[d]		
$\omega(1680)\to A_2\pi$	$(\frac{1600}{3})^{1/2}S_3$	+17	+17[d]	+17[d]		
$\omega(1680)\to[(\pi\pi)_\rho(\pi\pi)_\rho]_{P,1}$		−3.1	−3.2	−4.1		
$\omega(1680)\to[(\pi\pi)_\rho(\pi\pi)_\rho]_{F,1}$		−3.5	−4.0	−5.0		
$\omega(1680)\to[\omega\omega]_{P,1}$		−3.1	−3.2	−4.2		
$\omega(1680)\to[\omega\omega]_{F,1}$		−0.8	−0.8	−1.1		
This state can also decay via $\delta\pi,\epsilon\eta$						
$\phi(1890)\to[(K\pi)_{K^*}\bar{K}]_P$	$-(\frac{40}{9})^{1/2}P_5$	−5.6	−5.9	−7.2		c
$\phi(1890)\to[(K\pi)_{K^*}\bar{K}]_F$	$-(\frac{3}{20})^{1/2}F_1$	−3.7	−3.7	−3.3		c
$\phi(1890)\to Q_1\bar{K}$	0	+1.4	+1.4[d]	+1.4[d]		c,g
$\phi(1890)\to Q_2\bar{K}$	$(\frac{2}{3})^{1/2}D_5$	+0.9	+0.9[d]	+0.9[d]		c,g
$\phi(1890)\to[(K\pi)_{K^*}(K\pi)_{\bar{K}^*}]_{P,1}$		−3.0	−3.1	−3.8		
$\phi(1890)\to[(K\pi)_{K^*}(K\pi)_{\bar{K}^*}]_{F,1}$		−1.2	−1.2	−1.2		
This state can also decay via $\kappa\bar{K},\epsilon_s\eta,A_1\pi,A_2\pi,\rho\rho$						
$1\,^3D_1$: $J^{PC_n}=1^{--}$						
$\rho(1660)\to\pi\pi$	$-(\frac{40}{9})^{1/2}P_5$	−5.9	−6.1	−8.5	See IV B	
$\rho(1660)\to\pi_r\pi$		+7.9	+8.1	+3.1	See IV B	j
$\rho(1660)\to\omega\pi$	$-(\frac{20}{9})^{1/2}P_5$	−4.7	−4.9	−5.7	See IV B	
$\rho(1660)\to\omega_r\pi$		+1.4	+1.4	+0.1	See IV B	j
$\rho(1660)\to K\bar{K}$	$-(\frac{20}{9})^{1/2}P_5$	−5.5	−5.8	−6.9	See IV B	
$\rho(1660)\to(\pi\pi)_\rho\eta$	$-(\frac{10}{9})^{1/2}P_5$	−2.7	−2.8	−3.2	See IV B	
$\rho(1660)\to(K\pi)_{K^*}\bar{K}$	$(\frac{10}{9})^{1/2}P_5$	+2.9	+3.0	+3.4	See IV B	c

TABLE II. (*Continued*).

Decay	(1) Amplitude	(2) γ^0_{00}=const [Case (ii)]	(3) Flux tube [Case (ii)]	(4) Flux tube [Case (i)]	(5) Experiment[a]	(6) Comments
$\rho(1660)\to H\pi$	$\frac{40}{3}S_3$	+9.9	+9.9[d]	+9.9[d]	See IV B	
$\rho(1660)\to A_1\pi$	$\frac{40}{3}S_3$	+9.4	+9.4[d]	+9.4[d]	See IV B	
$\rho(1660)\to[(\pi\pi)_\rho(\pi\pi)_\rho]_{P,2}$		+1.4	+1.5	+1.7	See IV B	
$\rho(1660)\to[(\pi\pi)_\rho(\pi\pi)_\rho]_{F,2}$		+3.1	+3.1	+3.5	See IV B	
$\rho(1660)\to[(\pi\pi)_\rho(\pi\pi)_\rho]_{P,0}$		−1.6	−1.6	−2.0	See IV B	
This state can also decay via $A_2\pi,\rho\epsilon$						
$\omega(1660)\to(\pi\pi)_\rho\pi$	$(\frac{20}{3})^{1/2}P_5$	+7.7	+8.0	+9.0	See IV B	
$\omega(1660)\to\rho_r\pi$		−3.1	−3.3	−0.04	See IV B	j
$\omega(1660)\to\omega\eta$	$-(\frac{10}{9})^{1/2}P_5$	−3.3	−3.4	−3.8	See IV B	
$\omega(1660)\to\omega\eta'$	$-(\frac{10}{9})^{1/2}P_5$	+1.5	+1.5[d]	+1.5[d]	See IV B	
$\omega(1660)\to K\bar{K}$	$-(\frac{20}{9})^{1/2}P_5$	−5.9	−6.2	−7.4	See IV B	
$\omega(1660)\to(K\pi)_{K^*}\bar{K}$	$(\frac{10}{9})^{1/2}P_5$	+3.1	+3.2	+3.6	See IV B	c
$\omega(1660)\to B\pi$	$-(\frac{1600}{3})^{1/2}S_3$	−21	−21[d]	−21[d]	See IV B	
This state can also decay via $\omega\epsilon,H\eta,\rho\delta,\phi\eta$						
$\phi(1880)\to\phi\eta$	$(\frac{20}{9})^{1/2}P_5$	+4.5	+4.6	+5.4	See IV B	
$\phi(1880)\to K\bar{K}$	$(\frac{40}{9})^{1/2}P_5$	+7.1	+7.2	+11	See IV B	
$\phi(1880)\to(K\pi)_{K^*}\bar{K}$	$(\frac{20}{9})^{1/2}P_5$	+5.5	+5.6	+6.8	See IV B	c
$\phi(1880)\to Q_1\bar{K}$	$-\frac{40}{3}S_3$	−2.3	−2.3[d]	−2.3[d]	See IV B	c,g
$\phi(1880)\to Q_2\bar{K}$	$(\frac{800}{9})^{1/2}S_3$	+11	+11[d]	+11[d]	See IV B	c,g
$\phi(1880)\to[(K\pi)_{K^*}(K\pi)_{\bar{K}^*}]_{P,2}$		≈0	≈0	≈0	See IV B	
$\phi(1880)\to[(K\pi)_{K^*}(K\pi)_{\bar{K}^*}]_{F,2}$		−0.4	−0.4	−0.5	See IV B	
$\phi(1880)\to[(K\pi)_{K^*}(K\pi)_{\bar{K}^*}]_{P,0}$		≈0	≈0	≈0	See IV B	
This state can also decay via $\rho\pi,\rho_r\pi,\omega\eta,\omega\eta',B\pi$						
$K^*(1780)\to K\pi$	$-(\frac{10}{3})^{1/2}P_5$	−4.8	−4.9	−7.1	See IV B	
$K^*(1780)\to K_r\pi$		+4.2	+4.4	+1.6	See IV B	j
$K^*(1780)\to K\eta$	$\frac{-\sqrt{5}(1+\sqrt{2})}{3}P_5$	−5.7	−5.8	−7.5	See IV B	
$K^*(1780)\to K\eta'$	$\frac{\sqrt{5}(-1+\sqrt{2})}{3}P_5$	+0.9	+0.9	+1.0	See IV B	
$K^*(1780)\to(K\pi)_{K^*}\pi$	$-(\frac{5}{3})^{1/2}P_5$	−3.1	−3.7	−4.5	See IV B	
$K^*(1780)\to K_r^*\pi$		+1.3	+1.3	+0.06	See IV B	j
$K^*(1780)\to(K\pi)_{K^*}\eta$	$\frac{\sqrt{5}(-1+\sqrt{2})}{\sqrt{18}}P_5$	+0.6	+0.7	+0.8	See IV B	
$K^*(1780)\to(\pi\pi)_\rho K$	$(\frac{5}{3})^{1/2}P_5$	+3.2	+3.3	+3.9	See IV B	
$K^*(1780)\to\omega K$	$-(\frac{5}{9})^{1/2}P_5$	−2.2	−2.2	−2.6	See IV B	
$K^*(1780)\to\phi K$	$-(\frac{10}{9})^{1/2}P_5$	−2.8	−2.9	−3.2	See IV B	
$K^*(1780)\to Q_1\pi$	$(\frac{400}{3})^{1/2}S_3$	+2.7	+2.7[d]	+2.7[d]	See IV B	j,g
$K^*(1780)\to Q_2\pi$	$-(\frac{200}{3})^{1/2}S_3$	−16[a]	−16[d]	−16[d]	See IV B	j,g
$K^*(1780)\to HK$	$\frac{20}{3}S_3$	+3.8	+3.8[d]	+3.8[d]	See IV B	
$K^*(1780)\to A_1K$	$(\frac{200}{3})^{1/2}S_3$	+4.1	+4.1[d]	+4.1[d]	See IV B	
$K^*(1780)\to BK$	$(\frac{400}{3})^{1/2}S_3$	+7.4	+7.4[d]	+7.4[d]	See IV B	
$K^*(1780)\to DK$	$(\frac{200}{9})^{1/2}S_3$	+2.7	+2.7[d]	+2.7[d]	See IV B	

TABLE II. (*Continued*).

Decay	(1) Amplitude	(2) γ_{00}^0=const [Case (ii)]	(3) Flux tube [Case (ii)]	(4) Flux tube [Case (i)]	(5) Experiment[a]	(6) Comments
$K^*(1780)\to[(K\pi)_{K^*}(\pi\pi)_\rho]_{P,2}$		≈ 0	≈ 0	≈ 0	See IV B	
$K^*(1780)\to[(K\pi)_{K^*}(\pi\pi)_\rho]_{F,2}$		-3.4	-3.4	-3.9	See IV B	
$K^*(1780)\to[(K\pi)_{K^*}(\pi\pi)_\rho]_{P,1}$	0	0	0	0	See IV B	k
$K^*(1780)\to[(K\pi)_{K^*}(\pi\pi)_\rho]_{P,0}$		$+1.6$	$+1.6$	$+1.8$	See IV B	
$K^*(1780)\to[(K\pi)_{K^*}\omega]_{P,2}$		-0.7	-0.7	-0.9	See IV B	
$K^*(1780)\to[(K\pi)_{K^*}\omega]_{F,2}$		-1.1	-1.1	-1.1	See IV B	
$K^*(1780)\to[(K\pi)_{K^*}\omega]_{P,1}$	0	0	0	0	See IV B	k
$K^*(1780)\to[(K\pi)_{K^*}\omega]_{P,0}$		$+0.5$	$+0.5$	$+0.6$	See IV B	
This state can also decay via $K^*(1420)\pi, Kf$						
$2\,^3P_2$: $J^{PC_n}=2^{++}$						
$A_2(1820)\to\rho\pi$		-8.8	-9.4	-4.0	See IV C	j
$A_2(1820)\to\eta\pi$		$+4.2$	$+4.5$	$+0.1$	See IV C	j
$A_2(1820)\to K\bar{K}$		-4.4	-4.7	-0.2	See IV C	j
$A_2(1820)\to\eta'\pi$		$+3.4$	$+3.6$	$+0.6$	See IV C	j
$A_2(1820)\to K^*\bar{K}$		-3.7	-4.0	-1.0	See IV C	j,c
$f(1820)\to\pi\pi$		-6.9	-7.4	0.6	See IV C	j
$f(1820)\to K\bar{K}$		-4.4	-4.7	-0.2	See IV C	j
$f(1820)\to\eta\eta$		$+2.1$	$+2.3$	$+0.2$	See IV C	j
$f(1820)\to\eta'\eta$		-1.7	-1.8	-0.4	See IV C	j
$f(1820)\to K^*\bar{K}$		-3.7	-4.0	-1.7	See IV C	j,c
$f'(2040)\to\pi\pi$	0	≈ 0	≈ 0	≈ 0	See IV C	j
$f'(2040)\to K\bar{K}$		-6.2	-6.8	-1.5	See IV C	j
$f'(2040)\to\eta\eta$		$+3.1$	$+3.3$	$+0.5$	See IV C	j
$f'(2040)\to\eta'\eta$		-3.7	-3.9	-0.9	See IV C	j
$f'(2040)\to K^*\bar{K}$		$+6.9$	$+7.4$	$+4.6$	See IV C	j,c
$K^*(1940)\to K\pi$		$+5.1$	$+5.5$	$+0.3$	See IV C	j
$K^*(1940)\to K^*\pi$		-5.8	-6.3	-3.0	See IV C	j
$K^*(1940)\to\rho K$		-5.6	-6.0	-3.4	See IV C	j
$K^*(1940)\to\omega K$		$+3.2$	$+3.5$	$+2.0$	See IV C	j
$K^*(1940)\to K\eta$		-0.9	-1.0	$+0.06$	See IV C	j
$K^*(1940)\to K\eta'$		$+4.0$	$+4.3$	$+1.0$	See IV C	j
$K^*(1940)\to K^*\eta$		-5.2	-5.5	-2.8	See IV C	j
$2\,^3P_1$: $J^{PC_n}=1^{++}$						
$A_1(1820)\to[\rho\pi]_S$		-2.2	-2.2	-5.7	See IV C	j
$A_1(1820)\to[\rho\pi]_D$		-6.6	-7.1	-5.9	See IV C	j
$D(1820)\to[K^*\bar{K}]_S$		$+1.6$	$+1.8$	-0.8	See IV C	j,c
$D(1820)\to[K^*\bar{K}]_D$		-2.8	-3.0	-2.3	See IV C	j,c
$E(2030)\to[K^*\bar{K}]_S$		$+1.5$	$+1.4$	$+3.0$	See IV C	j,c
$E(2030)\to[K^*\bar{K}]_D$		$+5.1$	$+5.5$	$+4.9$	See IV C	j,c

TABLE II. (*Continued*).

Decay	(1) Amplitude	(2) γ^0_{00}=const [Case (ii)]	(3) Flux tube [Case (ii)]	(4) Flux tube [Case (i)]	(5) Experiment[a]	(6) Comments
$2\,^3P_1$ and $2\,^1P_1$ (strange)[g]: $J^P=1^+$						
$Q_1(1900)\to[K^*\pi]_S$		+0.5	+0.5	+1.6	See IV C	j
$Q_1(1900)\to[K^*\pi]_D$		−6.9	−7.4	−5.8	See IV C	j
$Q_1(1900)\to[\rho K]_S$		−0.7	−0.6	−2.4	See IV C	j
$Q_1(1900)\to[\rho K]_D$		+4.5	+4.7	+4.1	See IV C	j
$Q_1(1900)\to[\omega K]_S$		+0.3	+0.3	+1.3	See IV C	j
$Q_1(1900)\to[\omega K]_D$		−2.5	−2.7	−2.4	See IV C	j
$Q_2(1930)\to[K^*\pi]_S$		−1.9	−1.9	−4.2	See IV C	j
$Q_2(1930)\to[K^*\pi]_D$		−2.6	−2.7	−2.3	See IV C	j
$Q_2(1930)\to[\rho K]_S$		−0.8	−0.8	−2.1	See IV C	j
$Q_2(1930)\to[\rho K]_D$		−5.6	−5.9	−5.3	See IV C	j
$Q_2(1930)\to[\omega K]_S$		+0.4	+0.4	+1.2	See IV C	j
$Q_2(1930)\to[\omega K]_D$		+3.2	+3.4	+3.0	See IV C	j
$2\,^1P_1$: $J^{PC_n}=1^{+-}$						
$B(1780)\to[\omega\pi]_S$		+0.7	+0.6	+2.7	See IV C	j
$B(1780)\to[\omega\pi]_D$		−6.3	−6.7	−5.4	See IV C	j
$H(1780)\to[\rho\pi]_S$		−1.3	−1.3	−4.7	See IV C	j
$H(1780)\to[\rho\pi]_D$		+12	+12	+9.4	See IV C	j
$H'(2010)\to[\rho\pi]_S$	0	≈0	≈0	≈0	See IV C	j
$H'(2010)\to[\rho\pi]_D$	0	≈0	≈0	≈0	See IV C	j
$H'(2010)\to[K^*\bar{K}]_S$		−0.8	−0.8	−2.1	See IV C	j,c
$H'(2010)\to[K^*\bar{K}]_D$		+7.1	+7.5	+6.5	See IV C	j,c
$2\,^3P_0$: $J^{PC_n}=0^{++}$						
$\delta_2(1780)\to\eta\pi$		−2.6	−2.6	−5.7	See IV C	j
$\delta_2(1780)\to K\bar{K}$		+1.6	+1.6	+4.5	See IV C	j
$\delta_2(1780)\to\eta'\pi$		+0.8	+1.0	−2.9	See IV C	j
$\epsilon(1780)\to\pi\pi$		+6.1	+6.3	+11	See IV C	j
$\epsilon(1780)\to K\bar{K}$		+1.6	+1.6	+4.5	See IV C	j
$\epsilon(1780)\to\eta\eta$		−0.5	−0.3	−2.3	See IV C	j
$\epsilon_s(1990)\to\pi\pi$	0	≈0	≈0	≈0	See IV C	j
$\epsilon_s(1990)\to K\bar{K}$		+5.2	+5.4	+7.5	See IV C	j
$\epsilon_s(1990)\to\eta\eta$		−2.3	−2.3	−3.3	See IV C	j
$\kappa(1890)\to K\pi$		−4.5	−4.6	−7.3	See IV C	j
$\kappa(1890)\to K\eta$		+0.6	+0.6	+0.8	See IV C	j
$\kappa(1890)\to K\eta'$		+2.0	+1.8	−1.7	See IV C	j
$1\,^3F_4$: $J^{PC_n}=4^{++}$						
$\delta(2010)\to\rho\pi$	$(\frac{1}{28})^{1/2}G_1$	+3.6	+3.7	+3.7		j
$\delta(2010)\to\rho_r\pi$		+0.4	+0.4	+0.8		j
$\delta(2010)\to\eta\pi$	$-(\frac{1}{140})^{1/2}G_1$	−2.3	−2.4	−1.7		j
$\delta(2010)\to\eta_r\pi$		−0.3	−0.3	−0.4		j

TABLE II. (*Continued*).

Decay	(1) Amplitude	(2) γ^0_{00}=const [Case (ii)]	(3) Flux tube [Case (ii)]	(4) Flux tube [Case (i)]	(5) Experiment[a]	(6) Comments
$\delta(2010)\to K\bar{K}$	$(\frac{1}{140})^{1/2}G_1$	+2.1	+2.2	+1.4		j
$\delta(2010)\to\eta'\pi$	$-(\frac{1}{140})^{1/2}G_1$	−1.2	−1.2	−0.8		j
$\delta(2010)\to\eta_r'\pi$		−0.04	−0.04	+0.07		j
$\delta(2010)\to K^*\bar{K}$	$(\frac{1}{112})^{1/2}G_1$	+1.0	+1.1	+1.0		j,c
$\delta(2010)\to\pi_r\eta$		−0.07	−0.07	−0.2		j
$h\to\pi\pi$	$(\frac{3}{140})^{1/2}G_1$	+5.0	5.2	+3.4	6±1	j
$h\to K\bar{K}$	$(\frac{1}{140})^{1/2}G_1$	+2.2	+2.3	+1.5	1.3±0.4	j
$h\to\eta\eta$	$-(\frac{1}{560})^{1/2}G_1$	−0.9	−1.0	−0.7		j
$h\to\eta\eta'$	$-(\frac{1}{280})^{1/2}G_1$	−0.5	−0.6	−0.3		j
$h\to\eta'\eta'$	$-(\frac{1}{560})^{1/2}G_1$	−0.02	−0.02	−0.01		j
$h\to K^*\bar{K}$	$(\frac{1}{112})^{1/2}G_1$	+1.1	+1.1	+1.1		j,c
$h_s(2220)\to\pi\pi$	0	≈0	≈0	≈0		j
$h_s(2220)\to K\bar{K}$	$(\frac{1}{70})^{1/2}G_1$	+4.5	+4.6	+3.0		j
$h_s(2220)\to\eta\eta$	$-(\frac{1}{280})^{1/2}G_1$	−2.1	−2.1	−1.1		j
$h_s(2220)\to\eta\eta'$	$(\frac{1}{140})^{1/2}G_1$	+1.5	+1.5	+0.8		j
$h_s(2220)\to\eta'\eta'$	$-(\frac{1}{280})^{1/2}G_1$	−0.2	−0.2	−0.1		j
$h_s(2220)\to K^*\bar{K}$	$-(\frac{1}{56})^{1/2}G_1$	−2.9	−3.0	−2.6		j,c
$K^*(2060)\to K\pi$	$-(\frac{3}{280})^{1/2}G_1$	−3.3	−3.4	−2.2	4±1	j
$K^*(2060)\to K^*\pi$	$(\frac{3}{224})^{1/2}G_1$	+2.1	+2.2	+2.1		j
$K^*(2060)\to\rho K$	$(\frac{3}{224})^{1/2}G_1$	+1.9	+2.0	+2.0		j
$K^*(2060)\to\omega K$	$-(\frac{1}{224})^{1/2}G_1$	−1.0	−1.1	−1.1		j
$K^*(2060)\to K\eta$	$-\frac{1-\sqrt{2}}{\sqrt{560}}G_1$	+0.5	+0.5	+0.2		j
$K^*(2060)\to K\eta'$	$-\frac{1+\sqrt{2}}{\sqrt{560}}G_1$	−1.1	−1.1	−0.8		j
$K^*(2060)\to K^*\eta$	$-\frac{1+\sqrt{2}}{\sqrt{448}}G_1$	−1.3	−1.3	−1.2		j
$K^*(2060)\to K^*\eta'$	$-\frac{1-\sqrt{2}}{\sqrt{448}}G_1$	+0.03	+0.03	+0.02		j
Charmed Mesons						
$1\,^3S_1$: $J^P=1^-$						
$D^{*+}\to D^0\pi^+$	$(\frac{3}{2})^{1/2}P_1^{c\bar{d}}$	+0.28	+0.34	+0.31		j,l
$D^{*+}\to D^+\pi^0$	$(\frac{3}{4})^{1/2}P_1^{c\bar{d}}$	+0.21	+0.23	+0.21		j,l
$D^{*0}\to D^0\pi^0$	$-(\frac{3}{4})^{1/2}P_1^{c\bar{d}}$	−0.24	−0.29	−0.26		j,l
$1\,^3P_2$: $J^P=2^+$						
$K_c^*(2500)\to D\pi$	$-(\frac{3}{4})^{1/2}D_1^{c\bar{d}}$	−6.3	−6.7	−5.3		j,l
$K_c^*(2500)\to D^*\pi$	$-(\frac{9}{8})^{1/2}D_1^{c\bar{d}}$	−4.7	−4.8	−4.1		j,l

TABLE II. (*Continued*).

Decay	(1) Amplitude	(2) γ_{00}^0=const [Case (ii)]	(3) Flux tube [Case (ii)]	(4) Flux tube [Case (i)]	(5) Experiment[a]	(6) Comments
$1\,^3P_1$ and $1\,^1P_1$ (see footnote g): $J^P=1^+$						
$Q_{1c}(2440)\to[D^*\pi]_S$	$\sqrt{6}S_1^{c\bar{q}}$	-1.7	-1.9	-2.7		j,l
$Q_{1c}(2440)\to[D^*\pi]_D$	$(\frac{3}{4})^{1/2}D_1^{c\bar{q}}$	$+4.6$	$+4.5$	$+3.6$		j,l
$Q_{2c}(2490)\to[D^*\pi]_S$	$\sqrt{12}S_1^{c\bar{q}}$	$+16$	$+18$	$+28$		j,l
$Q_{2c}(2490)\to[D^*\pi]_D$	$-(\frac{3}{8})^{1/2}D_1^{c\bar{q}}$	$+0.58$	$+0.60$	$+0.50$		j,l
$1\,^3P_0$: $J^P=0^+$						
$\kappa_c(2400)\to D\pi$	$\sqrt{6}S_1^{c\bar{q}}$	-13	-15	-25		j,l

[a]Experimental results ($\sqrt{\Gamma}$) from Particle Data Group (Ref. 9) unless otherwise indicated; if the amplitude sign is known, it is shown explicitly as $+\sqrt{\Gamma}$ or $-\sqrt{\Gamma}$.
[b]See Ref. 10.
[c]Note that the total width to, e.g., $K^*\bar{K}+\bar{K}^*K$, is twice the width to $K^*\bar{K}$.
[d]In this case γ_{00}^0=const has been used.
[e]Isoscalar mixing would modify this result.
[f]The status of the E is in flux at this time as the old E was at least partly the newly discovered $\iota(1440)$. There have also been claims that the true 1^{++} state may be at a higher mass (see Ref. 12).
[g]$Q_B(L_B)$ amplitude listed under $Q_1(L_1)$; $Q_A(L_A)$ amplitude listed under $Q_2(L_2)$. The numerical results for Q_1 and Q_2 are for a nominal mixing angle of 45°: $Q_1=(\frac{1}{2})^{1/2}(Q_A+Q_B)$, $Q_2=(\frac{1}{2})^{1/2}(Q_A-Q_B)$; for the L and Q_c mixing angles, see Ref. 8.
[h]See Ref. 11.
[i]This zero corresponds to an angular momentum selection rule of our model.
[j]The full machinery of Appendix D has not been used for this decay since it is far from threshold.
[k]This corresponds to an SU(3)-symmetry selection rule.
[l]Columns (3) and (4) do not take into account effect like those in Eqs. (B5) and (B6).

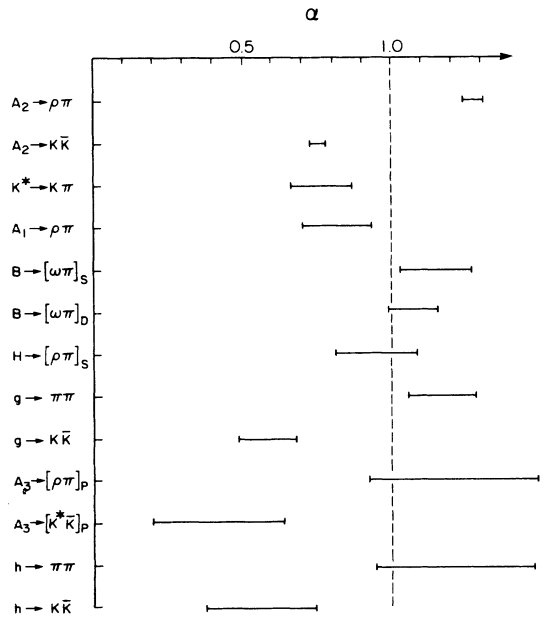

FIG. 5. A test of the sphericity of pair creation.

dence that the model will provide a reliable guide to the decay characteristics of as yet undiscovered mesons and to previously unobserved modes of known mesons. In addition, as will be discussed in our final section, the model's success makes it an excellent candidate for similar studies of baryons, hybrid mesons and baryons, and pure glue states.

IV. SOME REMARKS ON MESON PHENOMENOLOGY

There are a number of puzzles in the phenomenology of ordinary mesons which this analysis may help to illuminate.

A. The missing mesons of the quark model

The most straightforward of these puzzles involves the apparent absence of many of the meson states predicted by the quark model. As an illustration of the impact of our calculations on such puzzles, we will consider the fact that, in contrast with baryon spectroscopy, most of the mesons of the $L=2$ multiplets are missing. Our calculations normally supply an explanation for this state of affairs. Consider first the $^1D_2$ ($J^{PC}=2^{-+}$) nonet. The $I=1$ $A_3(1680)$ of this nonet is observed as one might have expected from our results: it has a predicted total width of about 200 MeV (as observed) of which a healthy

50% or so is predicted (as observed) to go through the simple channel $\rho\pi$. Its unseen $I=0$ nonstrange partner is considerably broader (its width is predicted to be about 400 MeV) and it decays almost totally to the relatively unexplored channel $A_2\pi$ with only about a 10% branching ratio to the simple channel $K^*\bar{K}+$c.c., so it is natural that it would be much more difficult to see than the $A_3(1680)$. The $s\bar{s}$ member of this nonet, which should be around 1900 MeV, is predicted to decay predominantly to $K^*\bar{K}+$ c.c. with a width of about 150 MeV and so should be observed in an experiment where it is produced; we presume that the absence of this state is in this case due to the difficulty of producing such an $s\bar{s}$ state. The strange $^1D_2$ and the nearby $^3D_2$ mesons are expected to be well mixed and overlapping resonances at about 1800 MeV with widths of about 300 MeV. The lower state is predicted to decay mainly to $Kf(1280)$ and ρK, while the upper state decays mainly to $K^*(1420)\pi$ and $K^*\pi$. This is probably consistent with the observed structures seen in the region of the $L(1770)$. Aside from this indication for at least a piece of the strange member of the $^3D_2$ nonet, it is otherwise unseen. With $J^{PC_n}=2^{--}$ its $I=1$ state can decay to $(A_2\pi)_S$ (unlike the corresponding $^1D_2$ state) and its broad width of about 500 MeV is dominated by this relatively unexplored four-pion final state. Its absence thus seems in order. The absence of the $I=0$ nonstrange $^3D_2$ state is, in contrast, rather odd. It should have a strong $\rho\pi$ branching ratio in a reasonable width of about 250 MeV. Apart from possible weak production, the only explanation we can offer in this case is that this state, which is expected to be nearly degenerate with the $A_3(1680)$, has been masked by the $\rho\pi$ decay mode of this well-established state. This could be checked by looking for a signal in the $\rho^0\pi^0$ channel. As for the $^1D_2$ $s\bar{s}$ state, we attribute the absence of the $^3D_2$ $s\bar{s}$ state to its being weakly produced, since it should be relatively narrow with a substantial $K^*\bar{K}+$ c.c. branching ratio.

In contrast with the $^1D_2$ and $^3D_2$ nonets, the members of the $^3D_3$ nonet are all known, so our discussion of the $L=2$ nonets can turn to the $^3D_1$ states. From the masses of the $^3D_3$ $g(1690)$ and $^1D_2$ $A_3(1680)$, it seems very likely (especially on comparing to the $L=1$ case) that the nonstrange $^3D_1$ states are near to 1680 MeV as predicted in Ref. 8. This immediately raises the question of the relation of, for example, the $I=1$ $^3D_1$ state to the well-established (but puzzling) $\rho(1600)$. We thus conclude this illustration of how our calculations may shed light on the missing meson resonances and turn to the discussion of the implications of our results for another, related puzzle in meson physics.

B. The excited-vector-meson puzzle

In most quark models the $J^{PC_n}=1^{--}$ $2\,^3S_1$ and $1\,^3D_1$ nonets coexist in the 1.4—1.9-GeV region. We have already pointed out that on empirical grounds the $I=1$ $1\,^3D_1$ state should be at about 1.68 GeV; various models predict the $I=1$ $2\,^3S_1$ state to be between about 1.4 and 1.6 GeV. Given that the $I=1$ $2\,^1S_0$ state (the π_r) is seen at about 1300 MeV, and the prejudice that the ρ_r-π_r splitting should be smaller than the ρ-π splitting since the radial excitations will have smaller values for their wave functions at the origin, these quark-model estimates seem reasonable. [Compare also to the known case of the $c\bar{c}$ $1\,^3D_1$ $\psi''(3770)$ and the $c\bar{c}$ $2\,^3S_1$ $\psi'(3685)$.] In the following discussion we will favor the $2\,^3S_1$ masses of the relativized quark model of Ref. 8 which lie at the lower end of the range of predictions, but the main thrust of our remarks will be seen to be independent of this choice.

The "vector-meson puzzle" which we address is compounded by the existence of uncertain and sometimes contradictory data, but one feature of the data which seems particularly odd is the existence of what appears to be an $s\bar{s}$ state [the $\phi(1680)$] just above the $I=1$ $\rho(1600)$ in contrast with the usual $s\bar{s}$-$(I=1)$ splittings of about 240 MeV. We consider this to be evidence in favor of a two-nonet structure for this region and would argue that all analyses of the vector mesons in this region must consider the possibility of broad, overlapping states in the data.

We now give our tentative interpretation of this region (which coincides very well with that of Ref. 8 based on their single-pion-emission model). From the known locations of the $^3D_3$ states $\omega(1670)$, $g(1690)$, and $\phi(1850)$ (whose decays are all well predicted by our model), and from that of the $^1D_2$ state $A_3(1680)$, it seems very likely to us that the $s\bar{s}$ $^3D_1$ state is to be found near 1900 MeV as predicted by Ref. 8. We are therefore driven to interpret the $\phi(1680)$ as the $s\bar{s}$ $2\,^3S_1$ state: its mass is almost exactly as predicted by Ref. 8 and its observed width and preference for $K^*\bar{K}+$c.c. are in accord with our predictions.

The nonstrange $I=1$ and $I=0$ and the strange $I=\frac{1}{2}$ sectors are messier, but we believe also consistent with our interpretation. From the spectroscopy of Ref. 8 and our decay analysis we expect in each of the first two cases a broad $2\,^3S_1$ state at around 1.45 GeV overlapping (and therefore interfering and mixing) with a very broad $1\,^3D_1$ state at around 1.66 GeV, not a single ρ' or ω' resonance as is often assumed. It is interesting to note that measurements of the properties of the $\rho'(1600)$ in different channels tend to give different results, perhaps indicating that there are important interference effects. In the $I=0$ sector little is known experimentally, but we expect a similar situation with the exception that in this case we have two *extremely* broad overlapping resonances (without mixing, $\Gamma_{1\,^3D_1}\gtrsim 600$ MeV, $\Gamma_{2\,^3S_1}\gtrsim 400$ MeV). Finally, in the strange sector we once again expect two broad overlapping resonances with masses, according to Ref. 8, of about 1.58 and 1.78 GeV. There is recent evidence[13] that there are indeed two states in this channel, lending further support to our picture of the "vector-meson puzzle." Nevertheless, the situation requires and deserves much more careful consideration than we have given it here: a full discussion would have to consider the possible mixings of these states via their decay channels, as well as interferences of the resonances with each other and with background amplitudes like those arising from the tails of the $1\,^3S_1$ states.

For other discussions of the vector-meson puzzle, some of which have elements in common with us, see Ref. 14.

C. Other radially excited mesons

For every value of L, the quark model predicts a sequence of radially excited states. These states, which are best known in the case of the $L=0$ $c\bar{c}$ and $b\bar{b}$ spectra, are characterized by the fact that the state $n\,^{2S+1}L_J$ has $n-1$ nodes (apart from $r=0$) in its radial wave function.

Such nodes will not have dramatic effects on the general characteristics of heavy $Q\bar{Q}$ states below $(Q\bar{q})+(q\bar{Q})$ threshold: the total hadronic widths of states like the $b\bar{b}$ P-wave sequence will depend only on the derivatives of their wave functions at the origin. (On the other hand, decay rates to exclusive channels below threshold may show more dramatic dependences on the nodal structure.) However, above threshold decays by pair creation can be dramatically influenced by radial nodes. This fact has been extensively discussed in both the light-quark vector mesons[14] (where it is responsible for some of the characteristics noted in the preceding section) and in the corresponding heavy-quark states.[15] We agree qualitatively with these results, and add to them our new results on the decays of $2P$ states. As shown in Table II, these decays often depend strongly on the choice of meson wave functions [compare columns (3) and (4)]: the nodes in the wave functions produce zeros in the decay amplitudes as a function of decay momentum q which are near to the physical values of q for many of the decays.

Although this means that our detailed predictions are untrustworthy for such decays, these results are nevertheless useful. They show that the intensity of radially excited states can sometimes show strong non-Breit-Wigner behavior, and that such states can appear with very different characteristics in different production and decay channels. They can also display strong nonphase-space violations of flavor symmetries between channels. This may complicate the identification of such states.

D. The scalar mesons

As our final illustration of a way in which our results may help to shed light on some old puzzles in meson spectroscopy, we turn to the scalar mesons. Our results in this sector confirm the conclusions drawn in Ref. 8 that the $q\bar{q}$ $1\,^3P_0$ scalar mesons are far too broad to be associated with the $S^*(975)$ and $\delta(980)$ mesons. If we try to associate $^3P_0$ $q\bar{q}$ states with these observed states (by assuming that the Ref. 8 mass predictions of 1090 MeV are too high and adjusting the available phase space accordingly), we predict $\Gamma(\delta\to\eta\pi)\simeq 250$ MeV and $\Gamma(S^*\to\pi\pi)\simeq 500$ MeV. This latter width, for example, is in stark contrast to the experimental value $\Gamma(S^*\to\pi\pi)\simeq 25$ MeV and this discrepancy seems even more outstanding when one recognizes that the decays of the other $L=1$ nonets (including several S-wave decays like these) are very well described by our model. We have checked that these conclusions are very stable under all variations of the model we have been able to imagine. We therefore suspect that the S^* and δ are not $q\bar{q}$ mesons.

A possible alternate interpretation of these same states has been given in Ref. 16: this study of the $q\,q\,\bar{q}\bar{q}$ system indicates that the $K\bar{K}$ system experiences an attraction from residual interquark forces that are probably strong enough to create weakly bound states. This picture of the δ and S^* as $K\bar{K}$ molecules immediately explains many of their other peculiar characteristics: (1) Unlike a pair of degenerate ideally mixed nonstrange mesons (e.g., ρ,ω), δ and S^* seem to couple preferentially to the $K\bar{K}$ system; (2) they are found just below $K\bar{K}$ threshold (like the deuteron is just below pn threshold); (3) they have very small widths to the open S-wave channels $\pi\pi$ and $\eta\pi$ because the reactions $K\bar{K}\to\pi\pi,\eta\pi$ occur very slowly since the $K\bar{K}$ system is very weakly bound.[16]

Note that this picture of the S^* and δ is closely related to an earlier suggestion in the context of the bag model,[17] though it avoids the problems of that picture with "fall apart" modes and as a bonus explains why these states happen to lie right at $K\bar{K}$ threshold. On the other hand, it is completely different from a recent explanation of this sector in terms of unitarity effects.[18] Indeed, in addition to disagreeing with the physical picture of Ref. 18, our calculation indicates that the meson form factors required by that model are unrealistic.

Any $q\,q\,\bar{q}\,\bar{q}$ explanations of the S^* and δ must, however, face another problem: where have the $q\bar{q}$ states gone? Our calculations provide an answer in agreement with that of Ref. 8 (to which we refer the interested reader for details). The total width of the $I=0$ $(u\bar{u}+d\bar{d})$ $1\,^3P_0$ state (ϵ) with its predicted mass would be of the order of 1000 MeV, and we associate this "resonance" with the slow rise of the S-wave $\pi\pi$ phase shift through 180° between threshold and 1.5 GeV *after subtracting off the* S^*. We predict the $I=1$ $1\,^3P_0$ state (δ_2) to have a width of the order of 500 MeV, consistent with the broad backgrounds seen in $\eta\pi$ production experiments. The $s\bar{s}$ $1\,^3P_0$ state (ϵ_s) is also predicted to be so broad that it would be very difficult to see, but in contrast we predict the $I=\frac{1}{2}$ state (κ) to have a width of the order of 300 MeV, consistent with the observed properties of the $\kappa(1350)$.

With these three examples we have only tried to illustrate the potential usefulness of the comprehensive decay analysis we have presented here. To the extent that the known and future successes of the model establish its credentials, it may eventually prove to be most useful not for meson spectroscopy as such, but rather in helping to distinguish the standard mesons of the quark model from more exotic objects like the possible $K\bar{K}$ bound states of Sec. IV D above, or from the hybrid mesons and glueballs which must eventually appear in the spectrum of QCD.

V. CONCLUSIONS

The flux-tube-breaking model has many attractive characteristics. Among these we should first remind the reader of a feature which came as a surprise to us: for the decays of ordinary relatively light mesons, its predictions are very similar to the successful $^3P_0$ model.[4,5] We count high among the accomplishments of this picture the fact that it explains this correspondence and thereby places this old phenomenological model on a much firmer footing within a QCD context. We have also been very impressed with the fact that the flux-tube-breaking model[19] can correctly reproduce (with an rms deviation of less than 25%) nearly a hundred well-known decay amplitudes

in terms of the single string-breaking amplitude γ_0. We confidently expect that the hundreds of additional amplitudes which we have predicted here will confirm the applicability of the model.

Over and above these successes of the model for ordinary meson decay is, in our opinion, its potential two-pronged utility in the study of new types of hadronic objects expected in QCD. Its first use, should it continue to describe ordinary mesons as well as presently indicated, will be as a guide (in conjunction with a spectroscopic work like that of Ref. 8) to ordinary mesons, so that we know when a hadronic object is something new and unexpected. Perhaps even more important, however, is the potential this model has to be extended to predict the hadronic couplings of hybrid mesons and glueballs. While there is little doubt that such objects should exist in QCD in the mass range from 1–2 GeV, any attempt to find them is severely compromised at the moment by the lack of solid predictions for their total and partial widths. The flux-tube-breaking model should be able to remedy this situation, especially for hybrid mesons:[20] unlike most other models of hadronic decay, it explicitly involves the gluonic degrees of freedom.

APPENDIX A: STRING OVERLAPS IN FLUX-TUBE BREAKING

In the flux-tube-breaking model for decays, not only must the two quark-antiquark pairs find themselves in the wave functions of the two final-state mesons, but also the two pieces of the broken flux tube ("string") of the original meson must find themselves in the string wave functions of their respective final state mesons. To study these string overlap integrals, we consider a "discrete" string with $n=0$ and $N+1$ fixed and with $n=1,2,\ldots,N$ each having a transverse degree of freedom $\mathbf{y}_n$.

A basis for the states of such a discrete string consists of the set of direct product states

$$|\,\mathbf{y}\rangle \equiv |\,\mathbf{y}_1\rangle\,|\,\mathbf{y}_2\rangle\cdots|\,\mathbf{y}_N\rangle \equiv |\,\mathbf{y}_1\mathbf{y}_2\cdots\mathbf{y}_N\rangle \tag{A1}$$

or alternatively, of the Fourier coefficients

$$\mathbf{a}_m=\sum_{n=1}^{N}\mathbf{y}_n\left[\frac{2}{N+1}\right]^{1/2}\sin\left[\frac{n\pi}{N+1}\right]m\ . \tag{A2}$$

If the "lattice spacing" of the discrete masses is a, then the Lagrangian is (in the small-oscillations approximation)

$$L\left[\mathbf{y},\frac{d\mathbf{y}}{dt}\right]=ba\sum_{n=0}^{N}\left[\frac{1}{2}\left[\frac{d\mathbf{y}_n}{dt}\right]^2-\frac{1}{2a^2}(\mathbf{y}_{n+1}-\mathbf{y}_n)^2\right] \tag{A3}$$

or alternatively

$$L\left[\mathbf{a},\frac{d\mathbf{a}}{dt}\right]=ba\sum_{m=1}^{N}\left[\frac{1}{2}\left[\frac{d\mathbf{a}_m}{dt}\right]-\tfrac{1}{2}\omega_m{}^2\mathbf{a}_m{}^2\right], \tag{A4}$$

where

$$\omega_m=\frac{2}{a}\sin\frac{\pi m}{2(N+1)}\ . \tag{A5}$$

Clearly the modes separate and the eigenstates of the discrete string can be labeled by mode occupation numbers n_m^α, where n is the number of "phonons" in the mth mode with polarization $\alpha=x,y$:

$$|\,n\rangle = |\,n_1^x n_1^y n_2^x n_2^y\cdots n_N^x n_N^y\rangle\ , \tag{A6}$$

$$E_n=\sum_{m=1}^{N}(n_m^x+n_m^y+1)\omega_m\ . \tag{A7}$$

The string wave function is correspondingly just the product wave function of the individual mode amplitudes:

$$\psi_n(\mathbf{a})=\psi_{n_1^x}(a_1^x)\psi_{n_1^y}(a_1^y)\cdots\psi_{n_N^x}(a_N^x)\psi_{n_N^y}(a_N^y)\ , \tag{A8}$$

where, for example,

$$\psi_{0_m^\alpha}(a_m^\alpha)=\frac{\alpha_m{}^{1/2}}{\pi^{1/4}}\exp[-\tfrac{1}{2}\alpha_m{}^2(a_m^\alpha)^2]\ , \tag{A9}$$

$$\psi_{1_m^\alpha}(a_m^\alpha)=\sqrt{2}\alpha_m a_m^\alpha\psi_{0_m^\alpha}(a_m^\alpha)\ , \tag{A10}$$

etc., are just the one-dimensional harmonic-oscillator wave functions, and

$$\alpha_m=\left[2b\sin\frac{\pi m}{2(N+1)}\right]^{1/2}\ . \tag{A11}$$

Before proceeding to the overlap integrals we require, it is instructive to examine a few properties of the string ground state. First we note that the rms deviation of the nth string element from its equilibrium position is

$$\langle\mathbf{y}_n{}^2\rangle_0{}^{1/2}=\left[\frac{2}{(N+1)b}\sum_{m=1}^{N}\frac{\sin^2\left[\dfrac{m\pi}{N+1}\right]n}{\sin\dfrac{m\pi}{2(N+1)}}\right]^{1/2}\ . \tag{A12}$$

At the center of the string this means that

$$\langle(\mathbf{y}_{\text{center}})^2\rangle_0{}^{1/2}=\left[\frac{2}{(N+1)b}\sum_{m=1}^{N}\frac{1}{\sin\dfrac{m\pi}{2(N+1)}}\right]^{1/2} \tag{A13}$$

so that as $N\to\infty$

$$\langle(\mathbf{y}_{\text{center}})^2\rangle_0^{1/2}\simeq\left[\frac{4}{\pi b}\ln\frac{2(N+1)}{\pi}\right]^{1/2}$$

$$\simeq\left[\frac{4}{\pi b}\ln N\right]^{1/2}\ . \tag{A14}$$

This divergence is symptomatic of the roughening transition which occurs as the number of normal modes be-

comes infinite. Since our string modes are to be cut off at the scale a_1 where $g(a_1)=1$ (namely, a_1 of the order of 0.1 fm) for all normal mesons $\ln N \simeq \ln r_{q\bar{q}}/a_1$ will be of the order of ln 10 and thus the rms excursion of the string center will be of the order of 1 fm. On the other hand, the rms value of the mean deviation $\bar{y}$ of the string from equilibrium

$$\bar{\mathbf{y}} \equiv \frac{1}{N}\sum_{n=1}^{N} \mathbf{y}_n \tag{A15}$$

is for large N finite and simply equal to

$$\langle \bar{y}^2 \rangle_0^{1/2} = \left[\frac{16}{\pi^3 b}\right]^{1/2} \simeq 0.4 \text{ fm} . \tag{A16}$$

We now turn to the string wave-function overlap amplitudes that are directly relevant to meson decay. The amplitude for a ground-state string to break at the point n_b, with displacement $\mathbf{y}_b$, into two other ground-state strings is

$$\gamma_{00}^0(n_b,\mathbf{y}_b) = \int d^2\mathbf{y}_1 \cdots d^2\mathbf{y}_N \delta^2(\mathbf{y}_{n_b}-\mathbf{y}_b) \langle 0_{L(n_b)} | \mathbf{y}_{1,L} \cdots \mathbf{y}_{n_b-1,L} \rangle \langle 0_{R(n_b)} | \mathbf{y}_{1,R} \cdots \mathbf{y}_{N-n_b,R} \rangle \langle \mathbf{y}_1 \cdots \mathbf{y}_N | 0 \rangle \tag{A17}$$

which is the formal expression for (the discrete version of) the string-breaking process depicted in Fig. 4(a). Note that

$$y_{n,L} = y_n - \left[\frac{n}{n_b}\right] y_b, \quad 0 \le n \le n_b , \tag{A18}$$

$$y_{n,R} = y_{n+n_b} - \left[\frac{N+1-n_b-n}{N+1-n_b}\right] y_b, \quad 0 \le n \le N-n_b+1 \tag{A19}$$

so that the left and right ground-state string wave functions are automatically referred to the equilibrium string positions, and

$$y_{0,L} = y_{n_b,L} = y_{0,R} = y_{N+1-n_b,R} = 0 .$$

Since the coordinates $\mathbf{y}_L$, $\mathbf{y}_R$, and $\mathbf{y}$ determine a set of Fourier coordinates $\mathbf{a}_L$, $\mathbf{a}_R$, and $\mathbf{a}$, we can write out (A17) in terms of the three ground-state wave functions:

$$\gamma_{00}^0(n_b,\mathbf{y}_b) = \int d^2\mathbf{y}_1 \cdots d^2\mathbf{y}_N \delta^2(\mathbf{y}_{n_b}-\mathbf{y}_b) \left[\frac{\alpha_{1,L} \cdots \alpha_{n_b-1,L}}{\pi^{(n_b-1)/2}}\right] \exp\left[-\tfrac{1}{2}\sum_{m=1}^{n_b-1} \alpha_{m,L}{}^2 \mathbf{a}_{m,L}{}^2\right]$$
$$\times \left[\frac{\alpha_{1,R} \cdots \alpha_{N-n_b,R}}{\pi^{(N-n_b)/2}}\right] \exp\left[-\tfrac{1}{2}\sum_{m=1}^{N-n_b} \alpha_{m,R}{}^2 \mathbf{a}_{m,R}{}^2\right] \left[\frac{\alpha_1 \cdots \alpha_N}{\pi^{N/2}}\right] \exp\left[-\tfrac{1}{2}\sum_{m=1}^{N} \alpha_m{}^2 \mathbf{a}_m{}^2\right] . \tag{A20}$$

These integrations can be done analytically; on inserting expressions like (A2) into (A20) one obtains

$$\gamma_{00}^0(n_b,\mathbf{y}_b) = A_{00}^0(n_b,N) \left[\frac{f(n_b,N)b}{\pi}\right]^{1/2} \exp[-\tfrac{1}{2} f(n_b,N) b y_b{}^2] , \tag{A21}$$

where A_{00}^0 and f are slowly varying functions of n_b and N of order unity. Note that the dimensionless function $\gamma_{00}^0(\mathbf{n})$ of Eq. (4) is proportional to $\gamma_{00}^0(n_b, \mathbf{y}_b)a$.

It is easily shown that decays involving excited strings have string overlap amplitudes closely related to (A21). They differ by the insertion of various factors of $\mathbf{a}_{m,L}$, $\mathbf{a}_{m,R}$, and $\mathbf{a}_m$ into (A17) as is appropriate to the wave functions (A8) involved. Indeed, such amplitudes are just equal to the same Gaussian factor appearing in (A21) multiplied by appropriate polynomials in $\mathbf{y}_b$.

APPENDIX B: THE $^3P_0$ DECAY AMPLITUDES

In the limit that the flux-tube wave function rms radius becomes infinite, the flux-tube model for ordinary meson decays goes over into the naive $^3P_0$ pair-creation model. In this extreme, if we approximate the meson wave functions by those of a harmonic oscillator, many decay amplitudes can easily be calculated analytically. These analytic results, which reveal the relationships which exist exist between various decays in a way that raw numerical results cannot, are displayed in column (1) of Table II in terms of certain basic amplitudes which we show in Table III below. Throughout this table we use the notation

TABLE III. The harmonic-oscillator $^3P_0$ amplitudes. These amplitudes are those of the harmonic-oscillator wave functions in the $^3P_0$ limit. The notation is defined in the text; our conventions for the harmonic-oscillator wave functions are those of Ref. 8.

Amplitude/A	Types of decay $A \to BC$
$S_1 = \left[1 - \frac{q^2}{4\beta^2}(1-\xi)(1+\xi)\right]$	$^3P_1 \to {}^3S_1 + {}^1S_0$, $^3P_0 \to {}^1S_0 + {}^1S_0$ $^1P_1 \to {}^3S_1 + {}^1S_0$
$S_2 = \left[(\frac{10}{3}\xi - 1) - \frac{q^2}{36\beta_A{}^2}(1+13\xi-20\xi^2) + \frac{q^4}{72\beta_A{}^4}(1+\xi)(1-\xi)^2\right]$	$2\,{}^3S_1 \to {}^3P_0 + {}^3S_1$, $2\,{}^3S_1 \to {}^3P_1 + {}^1S_0$ $2\,{}^3S_1 \to {}^1P_1 + {}^1S_0$
$S_3 = \frac{\beta^2}{\beta_A\beta_B}\left[1 - \frac{q^2}{4\beta^2}(1+\frac{2}{5}\xi+\frac{2}{5}\xi^2-\frac{9}{5}\xi^3) + \frac{q^4}{80\beta^2\beta_A{}^2}(1+\xi)(1-\xi)^2\right]$	$^3D_2 \to {}^3P_2 + {}^1S_0$, $^1D_2 \to {}^3P_2 + {}^1S_0$ $^3D_1 \to {}^3P_1 + {}^1S_0$, $^3D_1 \to {}^1P_1 + {}^1S_0$
$S_1^{ab} = \left[1 - \frac{q^2}{4\beta^2}(1-\xi_{ab})(1+\xi_{ab})\right]\frac{F_{ab}(q^2)}{F(q^2)}$	$^3P_1 \to {}^3S_1 + {}^1S_0$, $^1P_1 \to {}^3S_1 + {}^1S_0$ $^3P_0 \to {}^1S_0 + {}^1S_0$
$P_1 = \frac{q\beta_A}{\beta^2}(1+\xi)$	$^3S_1 \to {}^1S_0 + {}^1S_0$
$P_2 = \frac{q}{\beta_B}$	$^3P_1 \to {}^3P_0 + {}^1S_0$
$P_3 = \frac{q}{\beta_B}\left[(1-\frac{5}{2}\xi) + \frac{q^2}{8\beta_A{}^2}(1-\xi)(1+\xi)\right]$	$^1P_1 \to {}^3P_0 + {}^1S_0$
$P_4 = \frac{q\beta_A}{\beta^2}\left[(1+\frac{1}{3}\xi-\frac{10}{3}\xi^2) - \frac{q^2}{6\beta_A{}^2}(1+\xi)(1-\xi)^2\right]$	$2\,{}^1S_0 \to {}^3S_1 + {}^1S_0$, $2\,{}^3S_1 \to {}^1S_0 + {}^1S_0$ $2\,{}^3S_1 \to {}^3S_1 + {}^1S_0$
$P_5 = \frac{q}{\beta_A}\left[(1-\xi) - \frac{3q^2}{20\beta^2}(1+\xi)(1-\xi)^2\right]$	$^3D_2 \to {}^3S_1 + {}^1S_0$, $^1D_2 \to {}^3S_1 + {}^1S_0$ $^3D_1 \to {}^1S_0 + {}^1S_0$, $^3D_1 \to {}^3S_1 + {}^1S_0$
$P_1^{ab} = \frac{q\beta_A}{\beta^2}(1+\xi_{ab})\frac{F_{ab}(q^2)}{F(q^2)}$	$^3S_1 \to {}^1S_0 + {}^1S_0$
$D_1 = \frac{q^2}{\beta^2}(1+\xi)(1-\xi)$	$^3P_2 \to {}^1S_0 + {}^1S_0$, $^3P_2 \to {}^3S_1 + {}^1S_0$ $^3P_1 \to {}^3S_1 + {}^1S_0$, $^1P_1 \to {}^3S_1 + {}^1S_0$
$D_2 = \frac{q^2}{\beta_A\beta_B}\left[(1+\frac{20}{7}\xi-\frac{45}{7}\xi^2+\frac{18}{7}\xi^3) + \frac{3q^2}{28\beta_A{}^2}(1+\xi)(1-\xi)^2\right]$	$^3D_3 \to {}^1P_1 + {}^1S_0$
$D_3 = \frac{q^2\beta^2}{\beta_A{}^3\beta_B}\left[(1-4\xi+3\xi^2) - \frac{3q^2}{8\beta^2}(1+\xi)(1-\xi)^2\right]$	$^3D_3 \to {}^1P_1 + {}^1S_0$
$D_4 = \frac{q^2}{\beta_A\beta_B}(1-\xi)$	$^3D_2 \to {}^1P_1 + {}^1S_0$
$D_5 = \frac{q^2}{\beta_A\beta_B}(1-4\xi^2+3\xi^3)$	$^1D_2 \to {}^3P_1 + {}^1S_0$, $^1D_2 \to {}^1P_1 + {}^1S_0$

TABLE III. (*Continued*).

Amplitude/A	Types of decay $A\to BC$
$D_1^{ab}=\frac{q^2}{\beta^2}(1+\xi_{ab})(1-\xi_{ab})\frac{F_{ab}(a^2)}{F(q^2)}$	$^3P_2\to{}^1S_0+{}^1S_0$, $^3P_2\to{}^3S_1+{}^1S_0$
	$^3P_1\to{}^3S_1+{}^1S_0$, $^1P_1\to{}^3S_1+{}^1S_0$
$F_1=\frac{q^3}{\beta^2\beta_A}(1+\xi)(1-\xi)^2$	$^3D_3\to{}^1S_0+{}^1S_0$, $^3D_3\to{}^3S_1+{}^1S_0$
	$^3D_2\to{}^3S_1+{}^1S_0$, $^1D_2\to{}^3S_1+{}^1S_0$
$G_1=\frac{q^4}{\beta^2{\beta_A}^2}(1+\xi)(1-\xi)^3$	$^3F_4\to{}^1S_0+{}^1S_0$, $^3F_4\to{}^3S_1+{}^1S_0$

$$A\equiv\frac{8\gamma_0\pi^{3/4}}{9\beta^{1/2}}\left[\frac{\beta}{\beta_A}\right]^{5/2}\left[\frac{\beta^2}{\beta_B\beta_C}\right]^{3/2}F(q^2)\,, \tag{B1}$$

$$\beta^{-2}=\tfrac{1}{3}(\beta_A{}^{-2}+\beta_B{}^{-2}+\beta_C{}^{-2})\,, \tag{B2}$$

$$\xi=\beta^2/3\beta_A{}^2\,, \tag{B3}$$

$$F(q^2)=\exp\left[-\frac{q^2}{12}\left[\frac{\beta^2(\beta_B{}^2+\beta_C{}^2)}{2\beta_A{}^2\beta_B{}^2\beta_C{}^2}\right]\right], \tag{B4}$$

$$F_{ab}(q^2)=\exp\left[-\frac{q^2}{12}\left[\frac{\beta^2[\beta_C{}^2(1+\Delta_{ab})^2+\beta_B{}^2+\Delta_{ab}{}^2\beta_A{}^2]}{2\beta_A{}^2\beta_B{}^2\beta_C{}^2}\right]\right], \tag{B5}$$

$$\xi_{ab}=\xi\left[1-\Delta_{ab}\frac{\beta_A{}^2}{\beta_B{}^2}\right], \tag{B6}$$

where β_i is the (effective) harmonic-oscillator wave-function parameter for meson i and $\Delta_{ab}=(m_a-m_b)/(m_a+m_b)$ is a flavor-symmetry-breaking parameter which we have taken into account only in decays of charmed mesons.

In the simplest case one could take the above-mentioned harmonic-oscillator approximation to the meson wave functions to be described by a single parameter β which appears in the Gaussian factor $\exp(-\frac{1}{2}\beta^2r^2)$ multiplying polynomials in the usual harmonic-oscillator wave functions for the interquark coordinate $\mathbf{r}=\mathbf{r}_q-\mathbf{r}_{\bar{q}}$. This is the

TABLE IV. Helicity—partial-wave conversion factors. P and V represent pseudoscalar and vector particles, respectively, M_{λ_B} is used to represent $H^J_{\lambda_B\lambda_C}$, and M_L is used to represent M^J_{LS}, since $S_B=0$ in these simple cases.

J	Parity $(+)\to V+P$	Parity $(-)\to V+P$	Parity $(+)\to P+P$	Parity $(-)\to P+P$
0		$M_P=-M_0$	$M_S=M_0$	
1	$M_S=\sqrt{4/3}M_1+\sqrt{1/3}M_0$ $M_D=\sqrt{2/3}M_1-\sqrt{2/3}M_0$	$M_P=-\sqrt{2}M_1$		$M_P=M_0$
2	$M_D=-\sqrt{2}M_1$	$M_P=\sqrt{6/5}M_1+\sqrt{2/5}M_0$ $M_F=\sqrt{4/5}M_1-\sqrt{3/5}M_0$	$M_D=M_0$	
3	$M_D=\sqrt{8/7}M_1+\sqrt{3/7}M_0$ $M_G=\sqrt{6/7}M_1-\sqrt{4/7}M_0$	$M_F=-\sqrt{2}M_1$		$M_F=M_0$
4	$M_G=-\sqrt{2}M_1$	$M_F=\sqrt{10/9}M_1+\sqrt{4/9}M_0$ $M_H=\sqrt{8/9}M_1-\sqrt{5/9}M_0$	$M_G=M_0$	

approximation used in columns (2) and (3) of Table II. A somewhat more realistic approach is to allow β_i to vary from sector to sector by adjusting β_i in the harmonic-oscillator wave function to the rms relative momentum of the analogous state as calculated in a quark model (like that of Ref. 8) with realistic forces.

APPENDIX C: CONVERSION FROM HELICITY TO PARTIAL-WAVE AMPLITUDES

The formula (6) of the text directly provides expressions for helicity amplitudes $H^J_{\lambda_B\lambda_C}$. To convert to partial-wave amplitudes M^J_{LS} we use the Jacob-Wick formula

$$M^J_{LS}=\left[\frac{2L+1}{2J+1}\right]^{1/2}\sum_{\lambda_B\lambda_C} C_{LS}(JM;OM)C_{S_BS_C}(SM;\lambda_B,-\lambda_C)H^J_{\lambda_B\lambda_C}\ , \tag{C1}$$

where λ_B,λ_C and S_B,S_C are the final-state helicities and spins and where $M=\lambda_B-\lambda_C$, $\mathbf{S}=\mathbf{S}_B+\mathbf{S}_C$, and $\mathbf{J}=\mathbf{L}+\mathbf{S}$. The resulting factors for some simple cases are given in Table IV.

APPENDIX D: DECAY RATES

1. Phase-space factors

In a calculation using rest-frame wave functions, like this one, there are ambiguities surrounding the choice of phase space when the decays become relativistic. In particular, we know of no rigorous way of deriving the relationship between the formula (6) and a relativistic decay rate. The best way we know is the "mock-hadron" method of Refs. 8 and 21, but since the application of this method to all of Table II would be prohibitively laborious, our *prescription* here is to take

$$\Gamma[A\to(BC)_{LS}]=\frac{q}{(2J_A+1)\pi}\left[\frac{\tilde{M}_B\tilde{M}_C}{\tilde{M}_A}\right]|M^J_{LS}|^2 \tag{D1}$$

since in the weak-binding limit, where our results are valid, the decay rate would have this form with $\tilde{M}_i$ being the sum of the constituent-quark masses in meson i. Since we must contend with situations which are rather far from weak binding, we instead take $\tilde{M}_i$ to correspond to the calculated mass of the meson i in the spin-independent $q\bar{q}$ potential. (In this approximation, as examples, one has $\tilde{m}_\rho=\tilde{m}_\pi$ and $\tilde{m}_{A_2}=\tilde{m}_{A_1}=\tilde{m}_B=\tilde{m}_{\delta_2}$; we are thus building in the known approximate validity of SU(6) symmetry up to phase-space factors of q^{2L+1}.) A list of the $\tilde{M}_i$ is given in Table V; apart from some relatively small effects from annihilation and from the fact that the hyperfine interaction is too strong to be treated in lowest-order perturbation theory, these masses can be obtained from those quoted in Ref. 8 via the spin-averaging formula (for a meson flavor f with radial quantum number n, and orbital, spin, and total angular momenta L, S, and J)

$$\tilde{M}(fnL)=\frac{1}{4(2L+1)}\left[\sum_{m=-1,0,1}[2(L+m)+1]M(fnL;S=1,J=L+m)\right]+\tfrac{1}{4}M(fnL;S=0,J=L)\ . \tag{D2}$$

2. The effect of resonance widths

We next discuss the way we treat decays in which the narrow resonance approximation implied above is inadequate. This typically occurs for decays near threshold where a variation of the masses of the particles within their Breit-Wigner line shapes can produce significant variations in the available phase space. For example, the decay $A\to BC\to XYC$ can proceed for $M_A<M_B+M_C$ if Γ_B is very broad. In a few special cases, notably decays to the very broad $1\,^3P_0$ states, the effects of the widths are almost always significant. To take into account these effects we apply the result

TABLE V. $\tilde{M}_i$ values. The $I=0$ masses quoted are for ideally mixed states except in $1\,^1S_0$ where we quote the average of these two masses to represent the fully mixed η and η'.

Sectors	$I=1$	$I=0$ $u\bar{u}, d\bar{d}$	$I=0$ $s\bar{s}$	Strange $u\bar{s}$	Charmed $c\bar{u}$
$1\,^1S_0$	0.72	0.85	0.85	0.85	2.00
$1\,^3S_1$	0.72	0.72	0.98	0.85	2.00
$2\,^1S_0$, $2\,^3S_1$	1.41	1.41	1.68	1.55	
$1\,^1P_1$, $1\,^3P_0$, $1\,^3P_1$, $1\,^3P_2$	1.25	1.25	1.49	1.38	2.47
$2\,^1P_1$, $2\,^3P_0$, $2\,^3P_1$, $2\,^3P_2$	1.81	1.81	2.03	1.92	
$1\,^1D_2$, $1\,^3D_1$, $1\,^3D_2$, $1\,^3D_3$	1.68	1.68	1.90	1.79	

$$\Gamma_{A\to BC}(E_A)\propto \int d^3q\,|M(A\to BC)|^2 W_B(E_A-E_C,E_B)\ , \tag{D3}$$

where, with $\Gamma_i(E)$ the full energy-dependent width of i,

$$W_i(E,E')=\frac{\Gamma_i(E)/2\pi}{(E-E')^2+\dfrac{\Gamma_i(E)^2}{4}}\ . \tag{D4}$$

We use this result to calculate the branching ratio for $A\to(XY)_BC$ (the notation denotes that XY are the decay products of the resonance B) via

$$B(A\to(XY)_BC)\equiv\frac{\int dE_A\Gamma_{A\to BC}(E_A)W_A(E_A,M_A)}{\int dE_A\Gamma_A(E_A)W_A(E_A,M_A)}\ . \tag{D5}$$

The entries appearing in Table II are obtained by multiplying these branching ratios by $\Gamma_A(M_A)$, the full width of A at its nominal mass. Then if Γ_A is very small (D4) in conjunction with (D5) ensures that $\Gamma_{A\to BC}$ will be the nominal width at the resonance peak, but in general this result allows for decays in the upper part of the line shape of A to be considered. Note that (D3) is basically the sum of integrals over the (three-body) Dalitz plots for decays $A\to XYC$ over all the decay modes $B\to XY$. It therefore takes into account the effects of broad resonances and resonances with masses M_B which straddle the edge of the Dalitz plot in the variable M_{XY}.

If both final state particles B and C are broad we apply the straightforward generalization of (D5). For simplicity we have in all cases neglected the effects of possible interferences in the Dalitz plot.

ACKNOWLEDGMENT

We gratefully acknowledge continuous discussions with Jack Paton on the subjects of this paper.

[1]N. Isgur and J. Paton, Phys. Lett. **124B**, 247 (1983); Phys. Rev. D **31**, 2910 (1985).

[2]Hamiltonian lattice gauge theories were introduced via the SU(2) theory by J. Kogut and L. Susskind, Phys. Rev. D **11**, 395 (1975). For reviews of lattice gauge theories and calculations, see, for example, M. Bander, Phys. Rep. **75**, 206 (1981); J. Kogut, Rev. Mod. Phys. **55**, 775 (1983); L. Susskind, in *Weak and Electromagnetic Interactions at High Energies,* edited by R. Balian and C. H. Llewellyn-Smith (North-Holland, Amsterdam, 1977).

[3]For some early symmetry analyses, see H. J. Lipkin and S. Meshkov, Phys. Rev. Lett. **14**, 670 (1965); D. Faiman and A. W. Hendry, Phys. Rev. **173**, 1720 (1968); **180**, 1609 (1969); E. W. Colglazier and J. L. Rosner, Nucl. Phys. **B27**, 349 (1971); W. Petersen and J. Rosner, Phys. Rev. D **6**, 820 (1972); A. J. G. Hey, P. J. Litchfield, and R. J. Cashmore, Nucl. Phys. **B95**, 516 (1975); F. Gilman and I. Karliner, Phys. Rev. D **10**, 2194 (1974); J. Babcock and J. Rosner, Ann. Phys. (N.Y.) **96**, 191 (1976); J. Babcock *et al.*, Nucl. Phys. **B126**, 87 (1977); D. Faiman and D. E. Plane, *ibid.* **B50**, 379 (1972). For work on explicit decay models, see C. Becchi and G. Morpurgo, Phys. Rev. **149**, 1284 (1966); **140B**, 687 (1965); Phys. Lett. **17**, 352 (1965); A. N. Mitra and M. Ross, Phys. Rev. **158**, 1630 (1967); H. J. Lipkin, Phys. Rep. **8C**, 173 (1973); J. L. Rosner, *ibid.* **11C**, 189 (1974); R. Horgan, in *Proceedings of the Topical Conference on Baryon Resonances,* Oxford, 1976, edited by R. T. Ross and D. H. Saxon (Rutherford Laboratory, Chilton, England, 1977), p. 435; L. A. Copley, G. Karl, and E. Obryk, Phys. Lett. **29B**, 177 (1969); Nucl. Phys. **B13**, 303 (1969); D. Faiman and A. W. Hendry, Phys. Rev. **180**, 1572 (1969); Hohichi Ohta, Phys. Rev. Lett. **43**, 1201 (1979); R. G. Moorhouse, *ibid.* **16**, 771 (1966); R. P. Feynman, M. Kislinger, and F. Ravndal, Phys. Rev. D **3**, 2706 (1971); R. G. Moorhouse and N. H. Parsons, Nucl. Phys. **B62**, 109 (1973); R. Koniuk and N. Isgur, Phys. Rev. D **21**, 1868 (1980); see also Ref. 8.

[4]L. Micu, Nucl. Phys. **B10**, 521 (1961); see also Ref. 5.

[5]A. Le Yaouanc, L. Oliver, O. Pene, and J. C. Raynal, Phys. Rev. D **8**, 2223 (1973); **9**, 1415 (1974); **11**, 1272 (1975); M. Chaichian and R. Kogerler, Ann. Phys. (N.Y.) **124**, 61 (1980).

[6]R. Kokoski, Ph.D thesis, University of Toronto, 1984.

[7]J. Alcock and N. Cottingham, Z. Phys. C **25**, 161 (1984).

[8]S. Godfrey and N. Isgur, Phys. Rev. D **32**, 189 (1985).

[9]Particle Data Group, Rev. Mod. Phys. **56**, S1 (1984).

[10]F. Binon *et al.*, Nuovo Cimento **78A**, 313 (1983).

[11]W. Hoogland, in *New Flavours and Hadron Spectroscopy,* proceedings of the XVI Rencontre de Moriond, Les Arcs, France, 1981, edited by J. Tran Thanh Van (Editions Frontières, Dreux, France, 1981), p. 209; C. Daum *et al.*, Phys. Lett. **89B**, 276 (1980); **89B**, 281 (1980); **89B**, 285 (1980); Nucl. Phys. **B182**, 269 (1981); **B187**, 1 (1981).

[12]Ph. Gavillet *et al.*, Z. Phys. C **16**, 119 (1982).

[13]See, for example, A. Etkin *et al.*, Phys. Rev. D **22**, 42 (1980); D. Aston *et al.*, Phys. Lett. **149B**, 258 (1984).

[14]M. Böhm, H. Joos, and M. Krammer, Nucl. Phys. **B69**, 349 (1974); W. B. Kaufmann and R. J. Jacob, Phys. Rev. D **10**, 1051 (1974); A. Le Yaouanc *et al.*, Phys. Lett. **76B**, 484 (1978) and in Ref. 15; A. Bradley, J. Phys. G **4**, 1517 (1978). See also Refs. 5 and 8.

[15]A. Le Yaouanc *et al.*, Phys. Lett. **71B**, 397 (1977), and in Ref. 14; A. Bradley and D. Robson, Z. Phys. C **6**, 57 (1980). See also Ref. 5.

[16]J. Weinstein and N. Isgur, Phys. Rev. Lett. **48**, 659 (1982); Phys. Rev. D **27**, 588 (1983).

[17]R. L. Jaffe, Phys. Rev. D **15**, 267 (1977); **15**, 281 (1977); R. L. Jaffe and K. Johnson, Phys. Lett. **60B**, 207 (1976); R. L. Jaffe, Phys. Rev. D **17**, 1444 (1978).

[18]N. A. Tornqvist, Phys. Rev. Lett. **49**, 624 (1982). See also the discussion of this paper by N. N. Achasov, S. A. Devyanin, and G. N. Shestakov, Z. Phys. C **22**, 53 (1984).

[19]As implied, a similarly impressive set of amplitudes is produced by the old $^3P_0$ model [column (2) of Table II]. So far as we are aware, our calculation is the most extensive available and so emphasizes the success of such models.

[20]N. Isgur, R. Kokoski, and J. Paton, Phys. Rev. Lett. **54**, 869 (1985).

[21]C. Hayne and N. Isgur, Phys. Rev. D **25**, 1944 (1982).